

# Dynamic response of beams excited by moving oscillators: Approximate analytical solutions for general boundary conditions



Alberto Di Matteo

Dipartimento di Ingegneria, Università degli Studi di Palermo, Viale delle Scienze, I-90128 Palermo, Italy

## ARTICLE INFO

### Article history:

Received 20 May 2022

Accepted 30 January 2023

Available online 4 February 2023

### Keywords:

Closed-form solution

Vehicle-bridge interaction

Moving oscillator

General boundary conditions

Damping

## ABSTRACT

In this paper, the dynamic response of an Euler-Bernoulli beam with general boundary conditions (BCs) and subject to a moving oscillator is examined. Notably, novel approximate closed-form expressions are determined for the vertical responses of both the beam and the moving oscillator, specifically considering the effect of damping in these systems, commonly omitted in standard approaches in the literature. In this regard, a modal superposition procedure is adopted and combined with an appropriate expansion-based approach of the dynamic response of the system, which naturally arises considering the oscillator-beam mass ratio to be reasonably small. Further, general boundary conditions are treated exploiting the use of a suitable set of orthogonal polynomial functions as beam mode shapes. In this manner, novel direct expressions for the response of the system are derived, in which the mode shapes coefficients explicitly appear. This leads to a straightforward application of the proposed solution, irrespective of the chosen BCs. Several numerical examples are presented to assess the reliability and accuracy of the proposed approach, considering different cases of beam BCs, and moving oscillator's parameters. Results are validated by comparison with the data of finite element analyses, and numerical solutions of the complete system of governing equations.

© 2023 The Author. Published by Elsevier Ltd. This is an open access article under the CC BY license (<http://creativecommons.org/licenses/by/4.0/>).

## 1. Introduction

Over the past few decades, the dynamic behavior of beam-like structures subjected to moving systems, as for instance bridges excited by moving vehicles, has been an active field of research in structural mechanics. Notably, this topic has nowadays gained renewed attention among researchers in the field due to the applications in a wide range of current engineering problems, including railway bridges crossed by high-speed trains and indirect structural monitoring techniques. Several research efforts have been then devoted to the determination of efficient and accurate solutions to this problem, which is generally numerically demanding. In this regard, a comprehensive review of early works can be found in [1], while some more recent contributions are detailed in [2,3].

Generally, the dynamic behavior of beam-like structures under moving systems can be studied utilizing three main different models: the moving force model, the moving mass model, and the moving oscillator model. In the moving force model [4] the moving system is described by a force travelling over the beam, neglecting the interaction effects of the moving system's inertia and stiffness, thus representing the simplest, and probably most commonly

employed approach. This model, for instance, can capture some of the features of the dynamic behavior of bridges subjected to the action of moving vehicles, although it is strictly valid only when the vehicle response is not required, and for reasonably small mass of the vehicles. In this regard, recent contributions have extended the first results reported in [1], focusing on more sophisticated beam models, taking into account general boundary conditions (BCs), multi-span beams, discontinuities, and non-classically damped beams [5–8]. In this context, in [9] an analytical approach is described for determining the response of uniform beams under moving forces, with general boundary conditions and using complex modal analysis. Further, in [10] some closed-form expressions have been obtained for multi-span beams with general BCs subjected to concentrated moving forces, using Laplace transformation.

In the moving mass model, the moving system consists of a mass travelling over the beam. It therefore represents an improvement over the moving force model in capturing the behavior of a bridge crossed by moving vehicles, since in this case the inertia effects are taken into account. On the other hand, the stiffness of the moving system is assumed to be infinite and, therefore, the effects of the displacement of the moving body relative to the beam are not considered. Clearly, these effects may become particularly relevant in the presence of pavement roughness, and they

E-mail address: [alberto.dimatteo@unipa.it](mailto:alberto.dimatteo@unipa.it)

are required for the modern applications in structural monitoring based on vehicle-bridge interaction dynamics [11]. Some early contributions on this model can be found in [12–14], while more recently in [15] the vibration of non-uniform beams with different BCs has been investigated employing particular orthogonal polynomial functions generated using a Gram-Schmidt process.

As far as the moving oscillator model is concerned, it is generally regarded as the most accurate one, among the three aforementioned models, which can be used to study the dynamic interaction between a moving vehicle and the supporting bridge. It yields a more realistic description of the interaction effects between the moving systems and the beam, at the expense of increased difficulty and complexity in the solution of the problem. For this reason, several research efforts have been devoted to the analysis and efficient solution of this problem. In this regard, some contributions can be found in [1,11,16–19] dealing with methods for the analysis of simply-supported beams subjected to moving oscillators modeled as one degree-of-freedom (DOF) systems. For instance, in [11] approximate closed-form expressions have been derived for the response of a simply-supported beam crossed by a vehicle modeled as a one DOF oscillator. Note that, these solutions have been obtained approximately decoupling the originally coupled equations of motion, neglecting the damping effects in both the beam and the oscillator. Further, considering the complexity involved in the numerical solution of this problem, several papers have focused on its efficient numerical implementation also using Finite Element (FE) procedures [20–23]. Recently, more sophisticated models of moving oscillators have been studied in the literature, employing a higher number of DOFs, to capture more accurately the vehicle dynamics also in the context of railway bridges [24–26]. In this regard, vehicle modeled as a 2 DOF systems have been analyzed in [27], where the results in [11] have been extended and some approximate closed-form expressions have been derived for the response of a simply-supported beam, and in [28], where a semi-analytical approach has been presented for the dynamic response of non-classically damped beams with general BCs based on a dynamic sub-structuring technique. Finally, recently [29,30] an approximate analytical method has been proposed to decouple the analysis of bridges crossed by vehicles modeled as single or multi-degree-of-freedom systems, valid for vehicle-to-bridge stiffness ratios.

In this context, it is worth mentioning that current applications of the so-called vehicle-bridge interaction (VBI), related for instance to indirect structural health monitoring (SHM) approaches [31,32], has led to further renewed interest in this topic. Specifically, first results in [11] have shown that, under some circumstances, bridge frequencies could be detected by measuring the response of vehicles travelling over the bridge. Experimental verifications of these first analytical results have been reported in [32], and later many research efforts have been devoted to refining these procedures for extracting bridge frequencies [33–36], as well as damping and mode shapes [37–40]. Notably, this could pave the way towards the use of indirect low-cost techniques for SHM of civil infrastructures, thus showing that the problem of the vibration response of beam-like structures under moving systems could warrant further investigations.

On the base of the preceding conspectus, it is evident that to date most of the literature has dealt with efficient numerical or semi-analytical procedures for the solution of the problem, using models of the moving system of various complexities to appropriately account for the dynamic properties of the vehicle. On the other hand, less attention has been paid so-far to the development of analytical solutions for a direct determination of the response of the system, that could be employed for many different purposes.

Note that, as previously mentioned, approximate closed-form expressions have been reported only for the case of a simply-

supported beam subjected to a moving vehicle modeled as one DOF oscillator [11] or a two DOF system [27]. In these cases, the analyses have been carried out omitting the effect of the damping in both the beam and the vehicle, and approximately decoupling the originally coupled equation of motion assuming small vehicle mass. Clearly, although the effect of the damping of the beam may be negligible, vehicle damping may be high, and hence it may be not generally neglected. Nevertheless, this procedure has led to rather simple expressions that have highlighted the presence of the beam frequencies in the vehicle response for applications related to the VBI method.

To the best of author's knowledge, no further closed-form solutions have been presented in the literature for the analysis of beam-like structures under moving oscillators. Therefore, the solution to more general and common cases which could consider the presence of damping, as well as comprise different BCs, remains an open challenge and still need to be investigated.

On this base, in the present paper a procedure is introduced for the determination of approximate analytical expressions for the response of beams with general BCs subjected to a single DOF moving oscillator, taking into account the effect of damping. In this regard, a major novel contribution of the paper is related to the definition of the approximate closed-form solutions which have been derived, for the first time, for both the beam and the moving oscillator vertical displacements in time-domain, for any BC. Specifically, these expressions have been determined following an approach similar to the classical expansion/perturbation method, often employed in the analysis of nonlinear dynamical systems [41–43], assuming a small value of the ratio between the mass of the moving oscillator and the beam. In this manner, the originally coupled set of differential equations governing the response of the system has been approximately decoupled. Interestingly, it is shown that the zero-order approximation obtained with the proposed approach reverts to the case in [11,27], simply determined omitting the coupling term.

Further, the presence of general BCs has been treated appropriately exploiting the use of mode-shape functions of polynomial form, referred to as characteristic orthogonal polynomial (COPs), generally used for the vibration analysis of plates [15,44,45]. In this manner, simple expressions are derived which explicitly depend on the coefficients of the COPs, thus rendering the application of the proposed approach particularly straightforward for any chosen BC.

Several numerical examples are presented to show the reliability of the proposed procedure for various BCs, taking into account different beam's parameters as well as mass ratio velocities of the moving oscillator. Finally, the accuracy of the proposed approach is assessed through comparison with the results of the numerical solution of the original set of coupled differential equations, and data of FE analyses developed in the commercial software Abaqus.

Notably, the main aim of the paper is related to the determination of the responses of both the beam and the moving oscillator, which are derived analytically, albeit approximately, for any BC and taking into account the effect of damping. Further, the validity of the involved approximations is addressed for the different analyzed cases. Clearly, the aforementioned problem could be solved with reasonable efficiency using standard procedures for the numerical solutions of the governing differential equations. Nonetheless, the derived closed-form expressions can be particularly useful, not only for assessing the reliability of other numerical procedures, but for instance to perform computationally efficient stochastic analyses of the problem [46–48] when, as customary, the irregular road profile is modelled as a stochastic process [49]. Additionally, on this base, analytical solutions in frequency-domain could be also derived which may be leveraged in the con-

text of the modern indirect SHM techniques based on the VBI approach.

**2. Problem definition**

Consider an elastically supported Euler-Bernoulli beam of span  $L$  with constant bending stiffness  $EI$ , coefficient of viscous damping  $c$ , and mass per unit length  $\mu$ , as shown in Fig. 1. Left and right ends comprise a linear vertical spring of stiffness  $k_1$  and  $k_2$ , respectively, and a rotational spring of stiffness  $r_1$  and  $r_2$ , respectively. In this manner, this beam can be assumed as a more general and refined model with respect to the classical simply-supported beam often used in the literature to capture the dynamic response of bridges. Clearly, spring stiffnesses may assume values from zero to infinity, thus capturing many different boundary conditions (BCs), including clamped, simply-support, and possible stiffening effects that may occur in real circumstances. Further, the beam is crossed by a moving oscillator with constant speed  $v$ , as in Fig. 1, that may be used to capture the main feature of a vehicle moving over the bridge.

The moving oscillator is characterized by a mass  $m_v$ , spring stiffness  $k_v$ , and damping coefficient  $c_v$ , that takes into account the damping effect of the vehicle's suspension systems.

The equations of motion governing the transverse or vertical response of the beam and moving oscillator are [1,2,10]

$$\mu \ddot{w} + c \dot{w} + EI w^{IV} = f(x, t), \tag{1.a}$$

$$m_v \ddot{y} + c_v (\dot{y} - \dot{w}|_{x=\bar{x}}) + k_v (y - w|_{x=\bar{x}}) = 0, \tag{1.b}$$

where a dot over a variable stands for derivation with respect to time, apexes denote derivatives with respect to coordinate  $x$ , and  $\bar{x}(t) = vt$  is the contact point position. Further, in Eq. (1)  $w(x, t)$  is the vertical beam displacement at the point  $x$  and time  $t$ ,  $y(t)$  is the vertical displacement of the moving oscillator with respect to its static equilibrium position, and  $f(x, t)$  is the interaction force transmitted to the beam by the moving oscillator applied in  $\bar{x}$ . This force can be generally expressed as follows:

$$f(x, t) = \chi(t) [m_v g + c_v (\dot{y} - \dot{w}|_{x=\bar{x}}) + k_v (y - w|_{x=\bar{x}})] \delta(x - \bar{x}) \tag{2}$$

where  $\delta(x)$  is the Dirac's delta function, and  $\chi(t)$  is the window function defined as

$$\chi(t) = \begin{cases} 1 & \text{for } 0 \leq t \leq L/v \\ 0 & \text{for } t > L/v \end{cases} \tag{3}$$

Notably, taking into account Eq. (1.b), Eq. (2) can be equivalently rewritten as

$$f(x, t) = \chi(t) [m_v g - m_v \ddot{y}] \delta(x - \bar{x}) \tag{4}$$

which is more amenable for further manipulations.

As far as the BCs of Eq. (1) are concerned, taking into account the well-known relations for the shear force  $T = -EI w'''$  and the bending moment  $M = -EI w''$ , they can be expressed as follows [28]

$$\begin{aligned} k_1 w(0, t) &= -EI w'''(0, t) \\ r_1 w'(0, t) &= EI w''(0, t) \end{aligned} \tag{5}$$

for the left boundary ( $x = 0$ ), and

$$\begin{aligned} k_2 w(L, t) &= EI w'''(L, t) \\ r_2 w'(L, t) &= -EI w''(L, t) \end{aligned} \tag{6}$$

for the right boundary ( $x = L$ ). Further, zero initial conditions are assumed, implying that the beam is at rest when the oscillator enters from the left end of the beam. Clearly, this assumption merely simplifies the notation and does not affect the generality of the proposed procedure. However, note that when the beam rests on flexible vertical supports, appropriate modeling of the initial conditions of the beam are required. This is necessary to accurately capture the effect that may be caused by the arrival of the moving oscillator on the beam, which generally produces a jump in the beam's acceleration response in ( $t = 0$ ). Alternatively, the moving oscillator may be considered in equilibrium with the beam in ( $t = 0$ ), if the beam is not completely decoupled from the external environment. In this case, no acceleration jump occurs, however appropriate modeling of the approaching phase is required. Readers may refer to [28], and reference therein, for further discussion on this issue.

Following conventional modal analysis [1,18], the displacement function  $w(x, t)$  can be expressed approximately as a series expansion

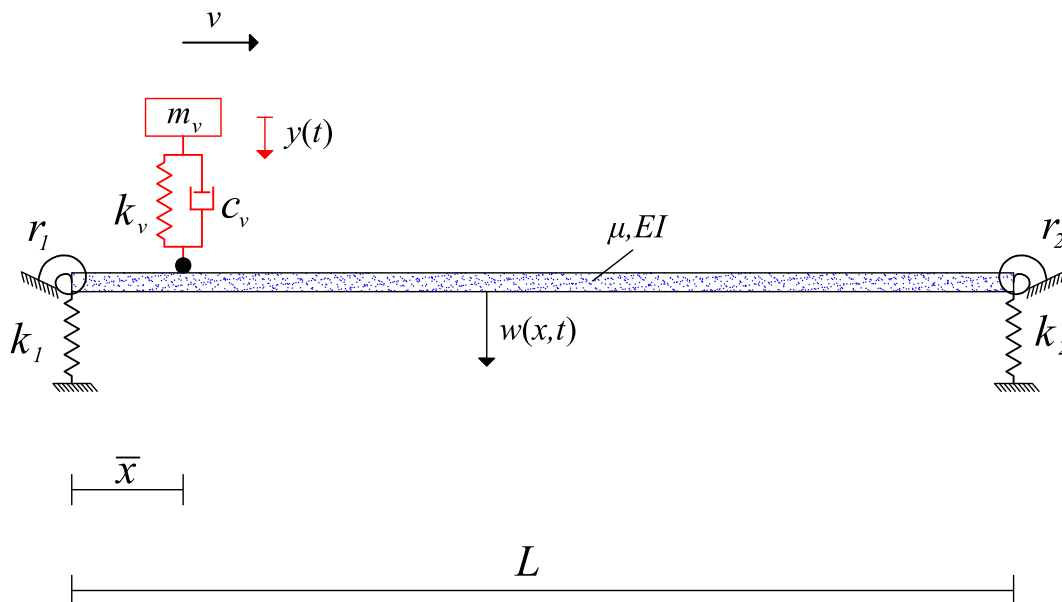


Fig. 1. Beam crossed by a moving oscillator.

sion in terms of the assumed first  $N$  mode shape functions  $\phi_j(x)$  of the beam, satisfying the beam BCs. Therefore,

$$w(x, t) \cong \sum_{j=1}^N q_j(t) \phi_j(x) \tag{7}$$

where  $q_j(t)$  is the  $j$ th modal displacement. Note that, as customary, the mode shapes  $\phi_j(x)$  of the unloaded and undamped beam can be evaluated as the solution of the following eigenproblem

$$\phi_j^{IV}(x) = \lambda_j^4 \phi_j(x), \quad j = 1, \dots, N \tag{8}$$

where  $\lambda_j^4 = \frac{\mu}{EI} \omega_j^2$ , and  $\omega_j$  is the angular frequency of vibration for the  $j$ th mode.

Substituting Eq. (7) into Eq. (1a), multiplying both sides by  $\phi_k(x)$ , and integrating with respect to  $x$  over the length of the beam, the equations of motion of the beam in terms of the modal displacements are

$$\ddot{q}_j(t) + 2\zeta_j \omega_j \dot{q}_j(t) + \omega_j^2 q_j(t) = \chi(t) \frac{\phi_j(\bar{x})}{\mu \int_0^L \phi_j^2(x) dx} [m_v g - m_v \ddot{y}(t)], \tag{9}$$

$j = 1, \dots, N$

where  $\zeta_j$  is the damping ratio of the  $j$ th mode, assuming the damping proportional to the mass [10]. It is worth mentioning that, Eq. (9) has been obtained using classical orthogonality conditions, that is

$$\int_0^L \phi_j(x) \phi_k(x) dx = 0, \quad \forall j \neq k \tag{10}$$

while the term  $\int_0^L \phi_j^2(x) dx$  has been kept at the right-hand side of Eq. (9) since it depends on the arbitrary chosen normalization condition.

Next, substituting Eq. (7) into Eq. (1b), and dividing by the mass  $m_v$ , the equation of motion of the moving oscillator can be obtained as

$$\ddot{y}(t) + 2\zeta_v \omega_v \dot{y}(t) + \omega_v^2 y(t) = 2\zeta_v \omega_v \sum_{j=1}^N \dot{q}_j(t) \phi_j(\bar{x}) + \omega_v \sum_{j=1}^N q_j(t) [\omega_v \phi_j(\bar{x}) + 2\zeta_v v \phi_j'(\bar{x})] \tag{11}$$

where  $\zeta_v$  and  $\omega_v$  are the damping ratio and natural frequency of the moving oscillator, respectively, and the following relation has been used

$$\dot{\phi}_j(\bar{x}(t)) = \frac{d\phi_j(\bar{x})}{d\bar{x}} \frac{d\bar{x}(t)}{dt} = v \phi_j'(\bar{x}) \tag{12}$$

Note that, Eqs. (9) and (11) represent a system of  $(N + 1)$  coupled differential equations, governing the response of both the beam and the moving oscillator. They are valid for general BCs and comprise the effects of damping in the beam as well as in the oscillator.

### 2.1. Formulation of the boundary conditions and classical mode shapes

As mentioned, mode shapes  $\phi_j(x)$  in Eqs. (9) depend on the specific BCs of the beam. In this regard, substituting Eq. (7) into Eqs. (5) and (6) yields the BCs in terms of mode shapes

$$\begin{aligned} k_1 \phi_j(0) &= -EI \phi_j'''(0) \\ r_1 \phi_j'(0) &= EI \phi_j''(0) \end{aligned} \tag{13}$$

for the left boundary ( $x = 0$ ), and

$$\begin{aligned} k_2 \phi_j(L) &= EI \phi_j'''(L) \\ r_2 \phi_j'(L) &= -EI \phi_j''(L) \end{aligned} \tag{14}$$

for the right boundary ( $x = L$ ), respectively. Further, the well-known solution of Eq. (8) can be written as [10]

$$\begin{aligned} \phi_j(x) &= A_j \cos(\lambda_j x) + B_j \sin(\lambda_j x) + C_j \cosh(\lambda_j x) \\ &\quad + D_j \sinh(\lambda_j x) \end{aligned} \tag{15}$$

generally referred to as the characteristic function of the beam, where  $A_j - D_j$  are the so-called mode shape coefficients. Next, differentiating Eq. (15) and applying the BCs in Eqs. (13) and (14), results in a set of algebraic equations that can be expressed in matrix form as

$$\Phi_{4 \times 4}(\lambda_j) \mathbf{J}_{4 \times 1} = 0 \tag{16}$$

where  $\Phi_{4 \times 4}$  is the characteristic matrix and  $\mathbf{J}_{4 \times 1}$  is a vector containing the mode shape coefficients as  $\mathbf{J} = [A_j \ B_j \ C_j \ D_j]^T$ . Clearly, these coefficients can be found as the eigenvectors of Eq. (16), while  $\lambda_j$  represents the corresponding eigenvalue, leading to the determination of the natural frequencies as  $\omega_j = \lambda_j^2 \sqrt{EI/\mu}$ .

As previously mentioned, mode shapes can be appropriately normalized according to an arbitrary chosen normalization condition. For instance, in many cases the mode shapes are mass-normalized, so that  $\mu \int_0^L \phi_j^2(x) dx = 1$ . However, as it will be shown in the following, it may be useful to normalize the mode shapes so that

$$\int_0^L \phi_j^2(x) dx = L \tag{17}$$

which can be easily done introducing a scale factor in the mode shape coefficients [10].

In this manner, employing these normalized mode shapes, and considering only the interval  $0 \leq t \leq L/v$ , Eqs. (9) and (11) become

$$\ddot{q}_j(t) + 2\zeta_j \omega_j \dot{q}_j(t) + \omega_j^2 q_j(t) = \alpha \phi_j(\bar{x}) - \varepsilon \phi_j(\bar{x}) \ddot{y}(t), \tag{18.a}$$

$j = 1, \dots, N$

$$\begin{aligned} \ddot{y}(t) + 2\zeta_v \omega_v \dot{y}(t) + \omega_v^2 y(t) &= 2\zeta_v \omega_v \sum_{j=1}^N \dot{q}_j(t) \phi_j(\bar{x}) \\ &+ \omega_v \sum_{j=1}^N q_j(t) [\omega_v \phi_j(\bar{x}) + 2\zeta_v v \phi_j'(\bar{x})] \end{aligned} \tag{18.b}$$

where  $\varepsilon = m_v/(\mu L)$  is a non-dimensional parameter, representing the oscillator-beam mass ratio, while  $\alpha = \varepsilon g$  has the dimension of an acceleration.

### 3. Dynamic response of the system

The equations of motion in Eq. (18), governing the response of the coupled system in Fig. 1, is a set of  $(N + 1)$  coupled linear differential equations, comprising time-dependent coefficients, which can be generally solved only through numerical procedures.

However, approximate analytical solutions could be obtained considering that in several circumstances the mass of the moving oscillator  $m_v$  is negligible compared to the total mass of the beam  $(\mu L)$ . Thus, the mass ratio  $\varepsilon$  is generally very small, that is  $\varepsilon \ll 1$ . In this manner, an analytical, albeit approximate, solution of Eq. (18) could be attempted following a procedure similar to the so-called standard perturbation approach, also referred to as straightforward expansion method [41], often employed in the analysis of nonlinear dynamical systems [42,43]. Therefore, the solution of Eq. (18) is approximately given in the form of an asymptotic expansion using  $\varepsilon$  as the perturbation parameter, that is

$$q_j(t) = q_j^{(0)}(t) + \varepsilon q_j^{(1)}(t) + \varepsilon^2 q_j^{(2)}(t) + O(\varepsilon^3), \quad j = 1, \dots, N \quad (19.a)$$

and

$$y(t) = y^{(0)}(t) + \varepsilon y^{(1)}(t) + \varepsilon^2 y^{(2)}(t) + O(\varepsilon^3) \quad (19.b)$$

where the apex in parentheses refers to the order of the approximation. In this manner, substituting Eq. (19) into Eq. (18), and equating coefficients of equal powers of  $\varepsilon$ , yields the following set of uncoupled linear differential equations.

**- Zero-Order**

$$\ddot{q}_j^{(0)} + 2\zeta_j \omega_j \dot{q}_j^{(0)} + \omega_j^2 q_j^{(0)} = \alpha \phi_j(\bar{x}), \quad j = 1, \dots, N \quad (20.a)$$

$$\begin{aligned} \ddot{y}^{(0)} + 2\zeta_v \omega_v \dot{y}^{(0)} + \omega_v^2 y^{(0)} &= 2\zeta_v \omega_v \sum_{j=1}^N \dot{q}_j^{(0)} \phi_j(\bar{x}) \\ + \omega_v \sum_{j=1}^N q_j^{(0)} [\omega_v \phi_j(\bar{x}) + 2\zeta_v v \phi_j'(\bar{x})] \end{aligned} \quad (20.b)$$

**- First-Order**

$$\ddot{q}_j^{(1)} + 2\zeta_j \omega_j \dot{q}_j^{(1)} + \omega_j^2 q_j^{(1)} = -\phi_j(\bar{x}) \ddot{y}^{(0)}, \quad j = 1, \dots, N \quad (21.a)$$

$$\begin{aligned} \ddot{y}^{(1)} + 2\zeta_v \omega_v \dot{y}^{(1)} + \omega_v^2 y^{(1)} &= 2\zeta_v \omega_v \sum_{j=1}^N \dot{q}_j^{(1)} \phi_j(\bar{x}) \\ + \omega_v \sum_{j=1}^N q_j^{(1)} [\omega_v \phi_j(\bar{x}) + 2\zeta_v v \phi_j'(\bar{x})] \end{aligned} \quad (21.b)$$

**- Second-Order**

$$\ddot{q}_j^{(2)} + 2\zeta_j \omega_j \dot{q}_j^{(2)} + \omega_j^2 q_j^{(2)} = -\phi_j(\bar{x}) \ddot{y}^{(1)}, \quad j = 1, \dots, N \quad (22.a)$$

$$\begin{aligned} \ddot{y}^{(2)} + 2\zeta_v \omega_v \dot{y}^{(2)} + \omega_v^2 y^{(2)} &= 2\zeta_v \omega_v \sum_{j=1}^N \dot{q}_j^{(2)} \phi_j(\bar{x}) \\ + \omega_v \sum_{j=1}^N q_j^{(2)} [\omega_v \phi_j(\bar{x}) + 2\zeta_v v \phi_j'(\bar{x})] \end{aligned} \quad (22.b)$$

Note that in Eqs. (20–22) the dependance on time  $t$  has been omitted for sake of conciseness, and they are valid only in the interval  $0 \leq t \leq L/v$ . Further, observe that, although  $\alpha$  depends on  $\varepsilon$ , the product  $(\alpha \phi_j(\bar{x}))$  is kept in the zero-order equation Eq. (20.a) since it is orders of magnitude greater than the last term at the right-hand-side of Eq. (18.a).

As it can be seen, while the equations related to  $q_j^{(p)}(t)$  (being  $p$  the order of the expansion) can be solved once the solution to the previous order  $y^{(p-1)}(t)$  is known, the response of the moving oscillator  $y^{(p)}(t)$  still depends on the solution of  $q_j^{(p)}(t)$ . Therefore, Eqs. (20–22) should be solved in sequence.

In passing, it should be mentioned that a similar reasoning has been firstly employed in [11] for the case of a simply-supported beam, following a rather heuristic approach in which Eq. (18.a) has been directly decoupled from Eq. (18.b), approximately omitting the last term at the right-hand-side of Eq. (18.a). In this manner, a solution has been derived for the much simpler case of a simply-supported undamped beam excited by a moving

undamped oscillator. Specifically, in [11] the response of the beam has been given as

$$w(x, t) = \sum_{j=1}^N \frac{\Delta_{st,j}}{1 - S_j^2} \left[ \sin \frac{j\pi x}{L} \left( \sin \frac{j\pi v t}{L} - S_j \sin \omega_j t \right) \right] \quad (23)$$

where  $\Delta_{st,j} = -2m_v g L^3 / (j^4 \pi^4 E I)$  is the static deflection caused by the vehicle with respect to the  $j$ th mode, while  $S_j = j\pi v / (L\omega_j)$  is a non-dimensional speed parameter. Analogous expressions have been given for the response of the moving oscillator, here omitted for sake of brevity. Clearly, these expressions are the solutions to the zero-order expansion in Eq. (20), in which all the terms containing the damping ratios of the mode shapes and of the moving oscillator are neglected.

**3.1. Zero-order response of the beam**

Analyzing Eq. (20.a), it can be observed that these represent the equations of motion of the modal displacements of a beam excited by a moving force. In this regard, pertinent closed-form solutions have been reported in [10] for general BCs, applying a Laplace transform approach, leading to rather unwieldy expressions for the beam displacements, not amenable for numerical implementation. In addition, the involved complexity would not allow for a straightforward determination of the moving oscillator's displacement, solving Eq. (20.b).

On this base, a different approach needs to be sought, which could lead to closed-form expressions for the responses of both the beam and the moving oscillator, not limited to the simply-supported case given in Eq. (23). Clearly, general direct expressions for the solutions to the zero-order expansion Eq. (20) could be obtained based on the use of the classical Duhamel's integral approach, as

$$q_0^{(j)}(t) = \alpha \int_0^t h_j(t - \tau) \phi_j(v\tau) d\tau \quad (24)$$

where

$$h_j(t) = \frac{1}{\omega_{d,j}} e^{-\zeta_j \omega_j t} \sin(\omega_{d,j} t) \quad (25)$$

in which  $\omega_{d,j}$  is the  $j$ th damped natural frequency  $\omega_{d,j} = \omega_j \sqrt{1 - \zeta_j^2}$ .

Note, however, that the integral in Eq. (24) cannot be easily solved employing the representation of the mode shapes in Eq. (15), since unwieldy expressions would be obtained for general BCs, as shown in [10] for the simple case of the moving force model.

Therefore, in this paper a different approach is proposed. Specifically, mode shapes in Eq. (15) are substituted with an appropriate set of orthogonal polynomials, as shown in [15,44,45], generally referred to as characteristic orthogonal polynomials (COPs). The first member of the set of COPs, that is  $\varphi_1(x)$ , is constructed as the polynomial of least degree satisfying all the boundary conditions of the beam. Therefore, a fourth-degree polynomial is introduced as

$$\varphi_1(x) = \sum_{k=0}^4 a_{1,k} x^k \quad (26)$$

where the coefficients  $a_{1,k}$  can be found by applying the pertinent BCs, as detailed in the Appendix A. Further, the following members of the COPs are generated by using a Gram-Schmidt process as

$$\varphi_2(x) = (x - P_2) \varphi_1(x) \quad (27.a)$$

$$\varphi_k(x) = (x - P_k) \varphi_{k-1}(x) - Q_k \varphi_{k-2}(x); \quad k = 3, 4, \dots \quad (27.b)$$

where

$$P_k = \frac{\int_0^L x \varphi_{k-1}^2(x) dx}{\int_0^L \varphi_{k-1}^2(x) dx} \quad (28)$$

and

$$Q_k = \frac{\int_0^L x \varphi_{k-1}(x) \varphi_{k-2}(x) dx}{\int_0^L \varphi_{k-2}^2(x) dx} \quad (29)$$

Observe that, although  $\varphi_1(x)$  satisfies all the BCs, both geometric and natural, the other members of the orthogonal set satisfy only the geometric boundary conditions. Further, functions in Eq. (26) do not generally satisfy the condition in Eq. (17). Thus, in this case the appropriate set of COPs, employed for the solution of Eq. (24), can be defined as

$$\tilde{\phi}_j(x) = \sqrt{\frac{L}{\int_0^L \varphi_j^2(x) dx}} \varphi_j(x); \quad j = 1, \dots, N \quad (30)$$

Clearly, considering Eq. (26), mode shapes in Eq. (30) can be more conveniently represented as

$$\tilde{\phi}_j(x) = \sum_{k=0}^n a_{j,k} x^k; \quad j = 1, \dots, N \quad (31)$$

where  $n = (3 + j)$  and  $a_{j,k}$  are the coefficients of the polynomial in Eq. (30) representing the  $j$ th mode shape of the beam.

In this manner, Eq. (20.a) can be rewritten as

$$\ddot{q}_j^{(0)}(t) + 2\zeta_j \omega_j \dot{q}_j^{(0)}(t) + \omega_j^2 q_j^{(0)}(t) = \alpha \sum_{k=0}^n a_{j,k} (vt)^k, \quad j = 1, \dots, N \quad (32)$$

whose solution, based on Eq. (24), is

$$q_j^{(0)}(t) = \alpha \sum_{k=0}^n a_{j,k} v^k \theta_{j,k}(t) \quad (33)$$

where

$$\theta_{j,k}(t) = \int_0^t h_j(t - \tau) \tau^k d\tau \quad (34)$$

Notably, the convolution integral in Eq. (34) can be more simply determined than the one in Eq. (24), and is given as

$$\theta_{j,k}(t) = h_j(t) \gamma_{j,k}^{(R)}(t) + \frac{\zeta_j \omega_j h_j(t) + \dot{h}_j(t)}{\omega_{d,j}} \gamma_{j,k}^{(I)}(t) \quad (35)$$

in which  $\gamma_{j,k}^{(R)}(t)$  and  $\gamma_{j,k}^{(I)}(t)$  are, respectively, the real and imaginary part of  $\gamma_{j,k}(t)$ , defined as

$$\gamma_{j,k}(t) = \sigma_j^{-1-k} [\Gamma(1+k) - \Gamma(1+k, \sigma_j t)] \quad (36)$$

where  $\sigma_j = -\zeta_j \omega_j + i \omega_{d,j}$ , and  $\Gamma(\cdot, t)$  is the incomplete Gamma function [50].

The numerical evaluation of Eq. (36) can be rather time consuming. However, expressing  $\gamma_{j,k}(t)$  for different values of  $k$ , and after appropriate manipulation, the function  $\theta_{j,k}(t)$  can be easily determined using the following recursive relation

$$\theta_{j,k}(t) = -\frac{k}{\delta_j} \left[ 2\zeta_j \omega_j \theta_{j,k-1}(t) + \dot{\theta}_{j,k-1}(t) \right] + \frac{t^k}{\delta_j}; \quad k \geq 1 \quad (37)$$

where  $\delta_j = \zeta_j^2 \omega_j^2 + \omega_{d,j}^2$ , and the initial solution for  $k = 0$  is given as

$$\theta_{j,0}(t) = -\frac{1}{\delta_j} \left[ 2\zeta_j \omega_j h_j(t) + \dot{h}_j(t) \right] + \frac{1}{\delta_j} \quad (38)$$

Finally, taking into account Eqs. (7) and (33), the displacement response of the beam can be directly given as

$$w(x, t) \cong \alpha \sum_{j=1}^N \sum_{k=0}^n \tilde{\phi}_j(x) a_{j,k} v^k \theta_{j,k}(t); \quad n = 3 + j \quad (39)$$

Next, corresponding velocity and acceleration responses can also be obtained from Eq. (39) considering the derivatives of  $\theta_{j,k}(t)$  in Eq. (35). Specifically, performing these derivations directly yields

$$\dot{\theta}_{j,k}(t) = \dot{h}_j(t) \gamma_{j,k}^{(R)}(t) + h_j(t) \dot{\gamma}_{j,k}^{(R)}(t) + \frac{\zeta_j \omega_j \dot{h}_j(t) + \ddot{h}_j(t)}{\omega_{d,j}} \gamma_{j,k}^{(I)}(t) + \frac{\zeta_j \omega_j h_j(t) + \dot{h}_j(t)}{\omega_{d,j}} \dot{\gamma}_{j,k}^{(I)}(t) \quad (40)$$

and

$$\ddot{\theta}_{j,k}(t) = \ddot{h}_j(t) \gamma_{j,k}^{(R)}(t) + 2\dot{h}_j(t) \dot{\gamma}_{j,k}^{(R)}(t) + h_j(t) \ddot{\gamma}_{j,k}^{(R)}(t) + \frac{\zeta_j \omega_j \ddot{h}_j(t) + \dot{h}_j(t)}{\omega_{d,j}} \gamma_{j,k}^{(I)}(t) + 2 \frac{\zeta_j \omega_j \dot{h}_j(t) + \ddot{h}_j(t)}{\omega_{d,j}} \dot{\gamma}_{j,k}^{(I)}(t) + \frac{\zeta_j \omega_j h_j(t) + \dot{h}_j(t)}{\omega_{d,j}} \ddot{\gamma}_{j,k}^{(I)}(t) \quad (41)$$

where, taking into account Eq. (36), the derivatives of the real and imaginary parts of  $\gamma_{j,k}(t)$  are

$$\dot{\gamma}_{j,k}^{(R)}(t) = e^t \zeta_j \omega_j t^k \cos(t \omega_{d,j}) \quad (42.a)$$

$$\dot{\gamma}_{j,k}^{(I)}(t) = -e^t \zeta_j \omega_j t^k \sin(t \omega_{d,j}) \quad (42.b)$$

and

$$\ddot{\gamma}_{j,k}^{(R)}(t) = e^t \zeta_j \omega_j t^{k-1} [(k + t \zeta_j \omega_j) \cos(t \omega_{d,j}) - t \omega_{d,j} \sin(t \omega_{d,j})] \quad (43.a)$$

$$\ddot{\gamma}_{j,k}^{(I)}(t) = -e^t \zeta_j \omega_j t^{k-1} [(k + t \zeta_j \omega_j) \sin(t \omega_{d,j}) + t \omega_{d,j} \cos(t \omega_{d,j})] \quad (43.b)$$

### 3.2. Zero-order response of the moving oscillator

Once the dynamic response of the beam has been obtained, the dynamic behavior of the moving oscillator can be determined solving Eq. (20.b), that can be rewritten as

$$\ddot{y}^{(0)}(t) + 2\zeta_v \omega_v \dot{y}^{(0)}(t) + \omega_v^2 y^{(0)}(t) = \sum_{j=1}^N f_j(t) \quad (44)$$

where the function  $f_j(t)$  takes into account the interaction effects between the bridge and the moving oscillator and, considering Eq. (31), is defined as

$$f_j(t) = 2\zeta_v \omega_v \dot{q}_j^{(0)}(t) \tilde{\phi}_j(vt) + \omega_v q_j^{(0)}(t) \left[ \omega_v \tilde{\phi}_j(vt) + 2\zeta_v v \tilde{\phi}_j'(vt) \right] \quad (45)$$

Solution of Eq. (44) can be determined by the Duhamel's integral as

$$y^{(0)}(t) = \int_0^t h_y(t - \tau) \sum_{j=1}^N f_j(\tau) d\tau \quad (46)$$

where  $h_y(t)$  represents the impulse response function of the moving oscillator, given as

$$h_y(t) = \frac{1}{\omega_{d,v}} e^{-\zeta_v \omega_v t} \sin(\omega_{d,v} t) \quad (47)$$

in which  $\omega_{d,v}$  is the damped natural frequency of the oscillator, that is  $\omega_{d,v} = \omega_v \sqrt{1 - \zeta_v^2}$ .

Next, taking into account Eqs. (31) and (33) and substituting into Eq. (45) yields

$$\begin{aligned}
 f_j(t) &= 2\zeta_v \omega_v \alpha \sum_{k=0}^n \sum_{s=0}^n a_{j,k} a_{s,k} v^{k+s} t^s \dot{\theta}_{j,k}(t) \\
 &+ \omega_v^2 \alpha \sum_{k=0}^n \sum_{s=0}^n a_{j,k} a_{s,k} v^{k+s} t^s \theta_{j,k}(t) + \\
 2\zeta_v \omega_v \alpha \sum_{k=0}^n \sum_{s=0}^{n-1} (s+1) a_{j,k} a_{j,s+1} v^{k+s+1} t^s \theta_{j,k}(t)
 \end{aligned} \tag{48}$$

In this manner, Eq. (46) yields the approximate analytical displacement response of the moving oscillator considering damping and general BCs as

$$\begin{aligned}
 y^{(0)}(t) &= \omega_v^2 \alpha \sum_{j=1}^N \sum_{k=0}^n \sum_{s=0}^n a_{j,k} a_{j,s} v^{k+s} I_{j,k,s}^{(1)}(t) \\
 &+ 2\zeta_v \omega_v \alpha \sum_{j=1}^N \sum_{k=0}^n \sum_{s=0}^{n-1} (s+1) a_{j,k} a_{j,s+1} v^{k+s+1} I_{j,k,s}^{(1)}(t) \\
 &+ 2\zeta_v \omega_v \alpha \sum_{j=1}^N \sum_{k=0}^n \sum_{s=0}^n a_{j,k} a_{j,s} v^{k+s} I_{j,k,s}^{(2)}(t)
 \end{aligned} \tag{49}$$

where

$$I_{j,k,s}^{(1)}(t) = \int_0^t h_y(t-\tau) \tau^s \theta_{j,k}(\tau) d\tau \tag{50.a}$$

and

$$I_{j,k,s}^{(2)}(t) = \int_0^t h_y(t-\tau) \tau^s \dot{\theta}_{j,k}(\tau) d\tau \tag{50.b}$$

Notably, based on the expressions of the function  $\theta_{j,k}(t)$  given in a recursive form in Eqs. (37) and (38), explicit solutions of these integrals can be obtained. Specifically, evaluating Eq. (50.a) for different values of  $s$ , and exploiting the properties of convolution integrals, after several manipulations the function  $I_{j,k,s}^{(1)}(t)$  can be expressed recursively as

$$\begin{aligned}
 I_{j,k,s}^{(1)}(t) &= -\frac{k}{\delta_j} \left[ I_{j,k-1,s}^{(1)}(t) - s I_{j,k-1,s-1}^{(1)}(t) + \zeta_j \omega_j I_{j,k-1,s}^{(1)}(t) \right] \\
 &+ \frac{1}{\delta_j} \theta_{y,s+k}(t); \quad k \geq 1
 \end{aligned} \tag{51}$$

where

$$\theta_{y,s+k}(t) = \int_0^t h_y(t-\tau) \tau^{s+k} d\tau \tag{52}$$

whose solution is given as in Eqs. (37) and (38), appropriately substituting the coefficients appearing in  $h_y(t)$ . Note that appropriate terms required to initialize the recursive expression in Eq. (51) are reported in Appendix B for sake of conciseness. Finally, considering the properties of the derivatives of the convolution integral, Eq. (50.b) can be obtained in a straightforward manner as

$$I_{j,k,s}^{(2)}(t) = \dot{I}_{j,k,s}^{(1)}(t) - s I_{j,k,s-1}^{(1)}(t) \tag{53}$$

Note that all the above reported integrals do not depend on the employed BCs, since the pertinent coefficients  $a_{j,k}$  appear explicitly only in Eq. (49). Therefore, Eqs. (51)–(53) can be computed once beforehand, thus greatly expediting the analyses.

### 3.3. Higher-order responses

Once the vertical displacement of the moving oscillator  $y^{(0)}(t)$  has been determined, a more accurate approximate expression of the displacement response of the beam can be found considering the higher-order expansions in Eqs. (21) and (22). In this regard, taking into account only the first-order expansion, the terms

$q_j^{(1)}(t)$  can be obtained solving Eq. (21.a) that, as it can be seen, approximately comprises the additional effect of the moving oscillator on the vertical displacement of the beam, previously omitted in Eq. (20.a).

Note that, a direct closed-form solution for  $q_j^{(1)}(t)$  cannot be determined due to the rather complex expression for  $y^{(0)}(t)$  in Eq. (49). However, considering the above reported novel analytical solutions for  $y^{(0)}(t)$ , a simple Duhamel's integral approach can be pursued, thus leading to the solution of Eq. (21.a) as

$$q_j^{(1)}(t) = - \int_0^t h_j(t-\tau) \tilde{\phi}_j(v\tau) \dot{y}^{(0)}(\tau) d\tau \tag{54}$$

Clearly, based on Eq. (49), Eq. (54) can be also easily solved numerically employing the standard numerical discretization procedures of the convolution integral implemented in any computational software. Further, once  $q_j^{(1)}(t)$  has been obtained, the first-order response of the moving oscillator displacement  $y^{(1)}(t)$  can be evaluated solving Eq. (21.b) following a similar approach.

Finally, taking into account Eqs. (7), and (19.a), a more accurate solution of the displacement response of the beam, up to the first-order term, is approximately given as

$$w(x,t) \cong \sum_{j=1}^N \tilde{\phi}_j(x) \left[ q_j^{(0)}(t) + \varepsilon q_j^{(1)}(t) \right] \tag{55}$$

## 4. Applications

In this section, the reliability of the proposed solution for the interaction problem of a damped beam subjected to a moving oscillator is assessed. Specifically, the proposed approximate analytical solutions are here compared with those related to the complete system (reference solution), obtained numerically solving the coupled differential equations in Eq. (18). Several beam BCs have been examined, showing the ability of the proposed approach to capture efficiently the responses of the beam and the moving oscillator in the different cases. In addition, results of Finite Element (FE) method analyses are also presented as comparison for further validation of the considered approach. In this regard, note that FE data have been obtained in Abaqus software, modeling the entire system with 3D elements for improved accuracy, using a total of 15,556 solid elements for the beam. Clearly, sensitivity analyses have been previously performed for the FE solution to assess its reliability.

Note that, for each of the considered cases, numerical analyses have been carried out for different values of the beam's and moving oscillator's parameters to assess the range of validity of the proposed approximate solutions. In this regard a reference set of parameters has been assumed, considering those reported in [11]. Specifically, the following data have been used: beam cross-sectional area  $A = 2 \text{ m}^2$ , moment of inertia  $I = 0.12 \text{ m}^4$ , elastic modulus  $E = 27.5 \text{ GPa}$ , length  $L = 25 \text{ m}$ , modal damping ratios  $\zeta_j = 0.0025$  ( $j = 1, \dots, N$ ), mass per unit length  $\rho = 4800 \text{ kg/m}$ , mass of the moving oscillator  $m_v = 1200 \text{ kg}$  (corresponding to a mass ratio  $\varepsilon = 1\%$ ), spring constant  $k_v = 500 \text{ kN/m}$  (corresponding to a natural frequency  $\omega_v = 20.41 \text{ rad/s}$ ), damping ratio  $\zeta_v = 0.08$ , and velocity  $v = 5 \text{ m/s}$ .

### 4.1. Simply supported beam

Consider the case of a beam simply supported at both ends, crossed by a moving oscillator. This case has been thoroughly discussed in the literature, since it can capture the main features of a bridge excited by a moving vehicle. In this regard, some approxi-

mate analytical solutions have been reported in [11] for zero damping condition for both the beam and the oscillator.

As far as the application of the proposed procedure is concerned, the first mode shape can be determined as discussed in the Appendix A, and is given in Eq. (A.9).

In Fig. 2 the displacement response of the mid-span of the beam and of the moving oscillator are shown, considering the above reported set of parameters. Specifically, in Fig. 2(a) proposed approach approximate analytical solution (red line), obtained from Eq. (39) using  $N = 3$ , is compared with the reference solution, obtained by numerical integration of system of differential equations Eq. (18) assuming  $N = 5$  (black dots), and results of the enhanced first-order approximate solution in Eq. (55) (blue dashed line). For sake of completeness, data obtained with the solution proposed in [11], reported in Eq. (23), are also shown (blue dotted line). Analogous results are reported in Fig. 2(b) for the response of the moving oscillator.

As it can be seen, results of the proposed approximate analytical solutions closely agree with the numerical solution of the complete system, both in terms of displacement response of the beam and of the moving oscillator. Clearly, as expected, Eq. (55) yields a more

accurate solution with respect to Eq. (39). Further, small discrepancies can be observed with respect to the FEM data, and this is due to the inherent differences in the modelling procedure in Abaqus software. Nevertheless, FEM data closely follow numerical results, thus still assessing the accuracy of the proposed approach. Further, Fig. 2(a) shows that the approach in [11] yields almost identical results as those obtained by Eq. (35). On the other hand, Fig. 2(b) shows a higher degree of discrepancy in terms of moving oscillator's displacements between the solution in [11] and the numerical results of the complete systems, due to the inherent additional approximations involved in [11] related to the zero-damping condition.

To further assess the accuracy of the proposed approach, additional analyses have been carried out varying the mass and the velocity of the moving oscillator. Specifically, in Fig. 3 the responses of both the beam and the moving oscillator are reported for several values of the mass ratio  $\varepsilon$ , obtained varying the moving oscillator's mass  $m_b$ . Note that, since the proposed approach is based on the main assumption of reasonably small oscillator-beam mass ratio, these analyses have been carried out keeping

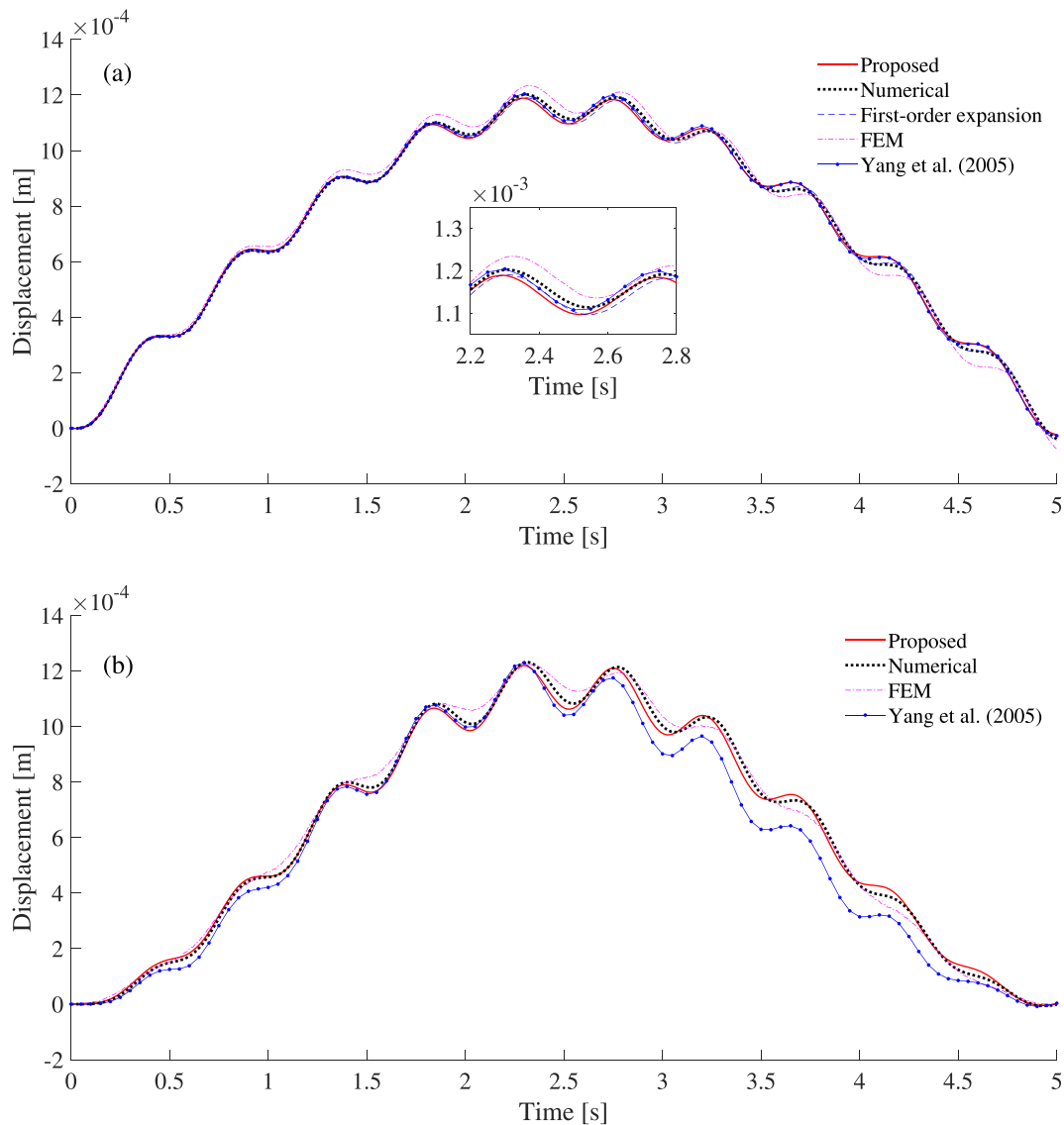


Fig. 2. Analysis for the case of a simply supported beam: (a) Displacement response of the mid-span of the beam; (b) Displacement response of the moving oscillator.



constant the value of  $\omega_v$ , to investigate only on the influence of the parameter  $\varepsilon$ .

As shown in Fig. 3, both the proposed analytical solution (red line), and the first-order expansion solution in Eq. (55) (blue dashed line), satisfactorily agree with the results of the numerical integration of the equations of motion Eq. (18) (black dotted line), for all the values of  $\varepsilon$ . Clearly, as expected, greater accuracy is achieved for smaller values of the mass ratio  $\varepsilon$ , especially in terms of the moving oscillator's displacements.

Analogous analyses have been carried out considering several values of the velocity of the moving oscillator (Fig. 4). As it can be seen, the proposed approach results adequately match the numerical data for all the considered values of velocity. Note that, data in Fig. 4 are shown in terms of the position of the oscillator on the beam to compare the results for several velocities.

An additional assessment on the accuracy of the proposed approach can also be given considering the plot of the maximum absolute displacement of the beam as a function of the velocity of the moving oscillator. This is shown in Fig. 5 for several values of the mass ratio  $\varepsilon$ . Again, it can be observed that the analytical

solutions lead to almost the same results of the numerical integration of Eqs. (18) for all the considered values of  $\varepsilon$ .

#### 4.2. Beam with rotational springs

Next, consider the case of a beam connected with rotational spring at both ends, characterized by equal rotational spring's constant  $r_1 = r_2 = r = 10^8 \text{ kN/rad}$ , and crossed by a moving oscillator. As far as the first mode shape in Eq. (31) is concerned, this is reported in Eq. (A.10) in the Appendix A. Note that this case reverts to the case of a simply-supported beam for  $r = 0$ , and to the case of a clamped-clamped beam for  $r \rightarrow \infty$ . Therefore, it may more accurately capture the behavior of a bridge crossed by a moving vehicle when possible natural degradation and damages occurring at the bridge supports are taken into account.

In Fig. 6 the displacement response of the mid-span of the beam and of the oscillator are shown. Specifically, in Fig. 6(a) the first-order expansion solution Eq. (55) (blue dashed line) is compared with the numerical solution of the equations of motion Eq. (18) (black dots), and the results of the approximate analytical solution

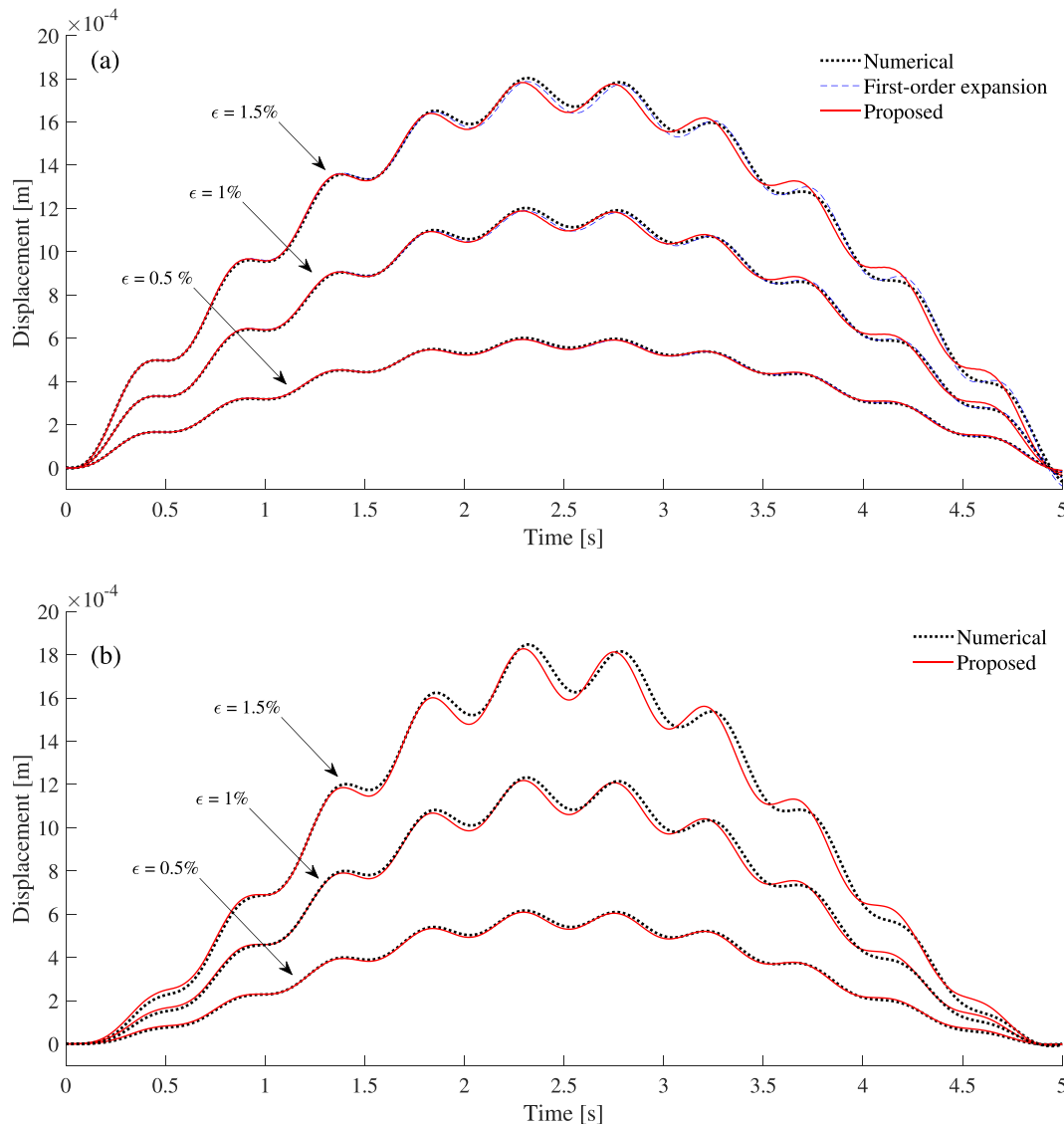


Fig. 3. Response for several values of the mass ratio (simply-supported beam): (a) Displacement response of the mid-span of the beam; (b) Displacement response of the moving oscillator.

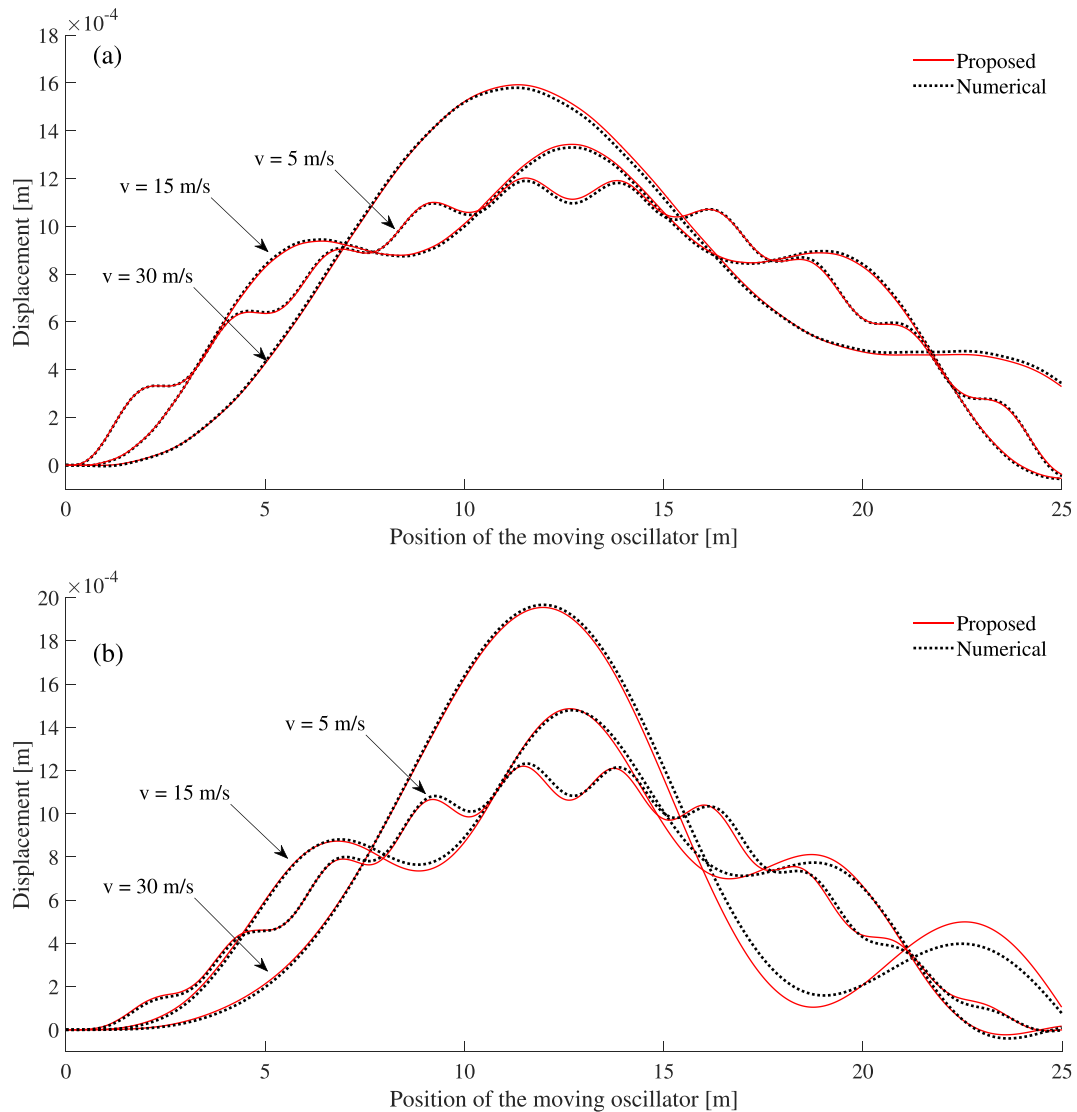


Fig. 4. Response for several values of moving oscillator's velocity (simply-supported beam): (a) Displacement response of the mid-span of the beam; (b) Displacement response of the moving oscillator.

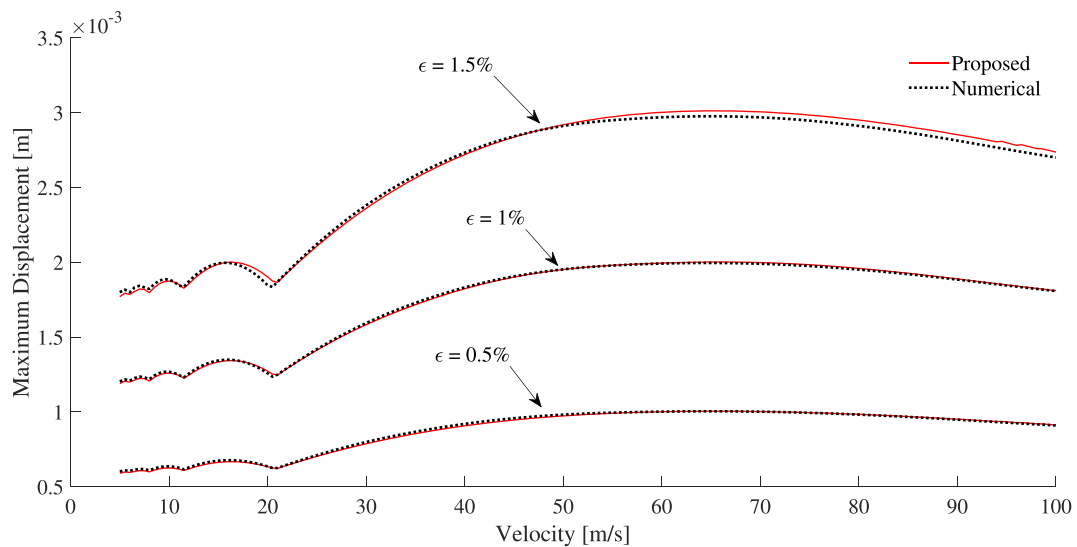


Fig. 5. Maximum displacement of the beam with simply-supported BCs, as a function of the velocity for various mass ratio values.

in Eq. (39) (red line). Analogous results are reported in Fig. 6(b) for the vertical displacement of the moving oscillator.

As it can be observed in these figures, results of the proposed approach closely agree with the numerical solution of the complete system, thus validating the reliability of the proposed method. Again, small differences can be observed with respect to the FEM data, and this is due to the inherent differences in the modelling procedure in Abaqus software. Nevertheless, FE data still closely follow numerical results, thus assessing the accuracy of the proposed approach. Further, again observe that the approximate analytical solution in Eq. (39) also leads to reasonably good results, although clearly Eq. (55) yields a more accurate solution.

Moreover, in Fig. 7 comparisons between the approximate analytical expressions (red line) and the numerical solutions of the complete system in Eqs. (18) (black dots) are reported for different values of the mass ratio  $\epsilon$ , again obtained keeping constant  $\omega_v$  while varying the mass of the moving oscillator  $m_v$ .

As it can be seen in Fig. 7, the proposed approach can generally capture the main features of the response of the system for all the values of  $\epsilon$ . Notably, very good accuracy is achieved for lower values of the mass ratio. On the other hand, accuracy decreases when the moving oscillator possess a larger mass, especially in terms of

$y(t)$ . Thus, from these analyses it can be argued that the considered approximate approach, and the related closed-form solutions, could be employed for oscillator-beam mass ratio  $\epsilon$  lower than 1 %. For higher values of  $\epsilon$ , numerical solutions or higher-order expansions would be required, especially for the response of the moving oscillator's displacement.

Further, an additional assessment on the accuracy of the proposed approach for several values of the mass ratio is given in Fig. 8. In this figure the maximum absolute displacement of the beam is reported as a function of the velocity of the moving oscillator. As it can be seen, the proposed approximate analytical solution in Eq. (39) leads to almost the same results of the numerical solution of Eqs. (18) for all the values of  $\epsilon$ .

Finally, analyses have been performed varying the rotational springs' constant  $r$ , aiming to assess the validity and accuracy of the approximate solution for different degree of stiffness of the BCs. Pertinent results are shown in Fig. 9, where analytical solutions (red lines) are juxtaposed with the numerical results of the complete system in Eqs. (18) (black dots).

As it can be seen, the approximate analytical solutions satisfactorily match the numerical results for all the values of spring con-

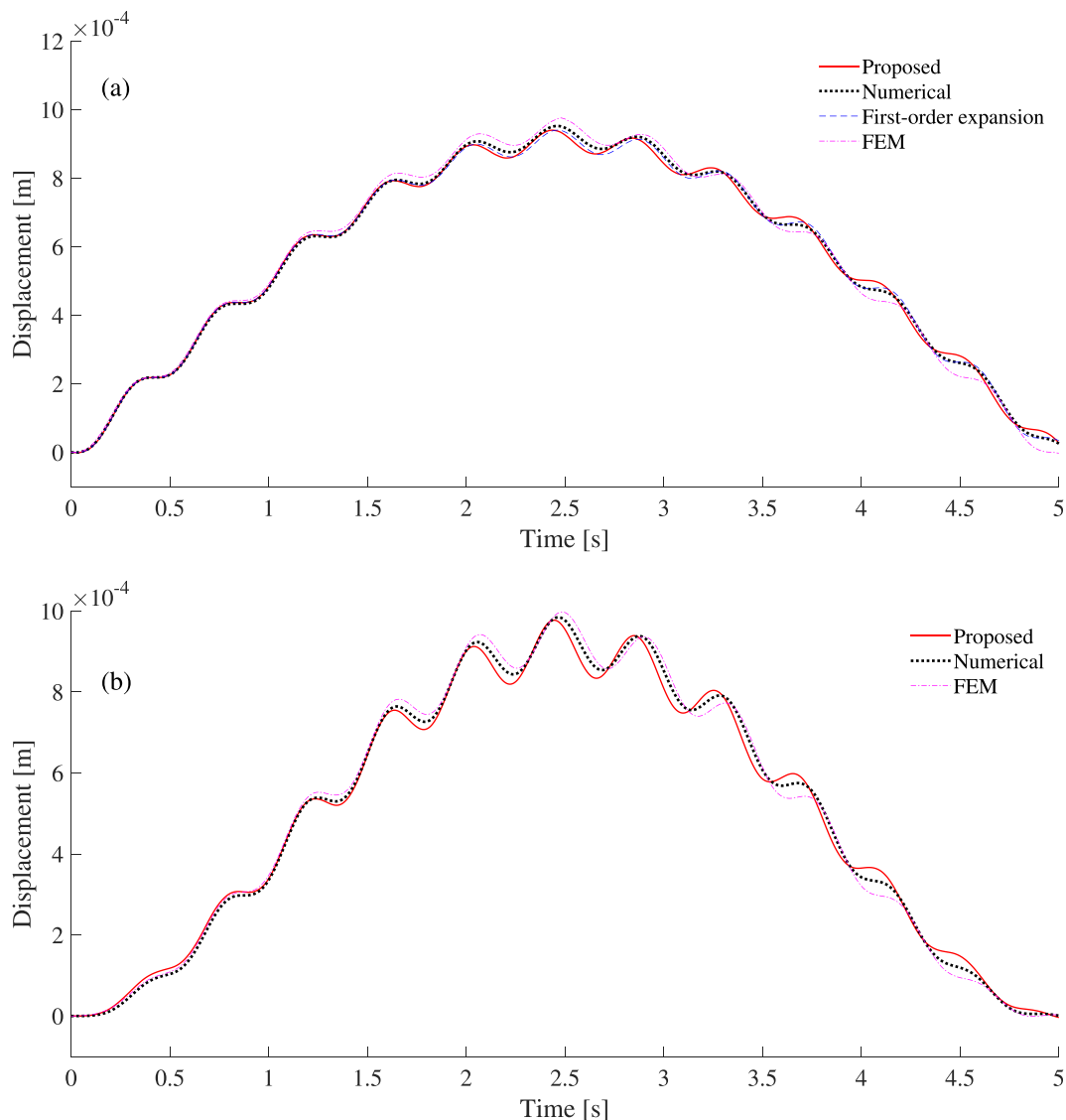


Fig. 6. Analysis for the case of a beam with rotational springs: (a) Displacement response of the mid-span of the beam; (b) Displacement response of the moving oscillator.

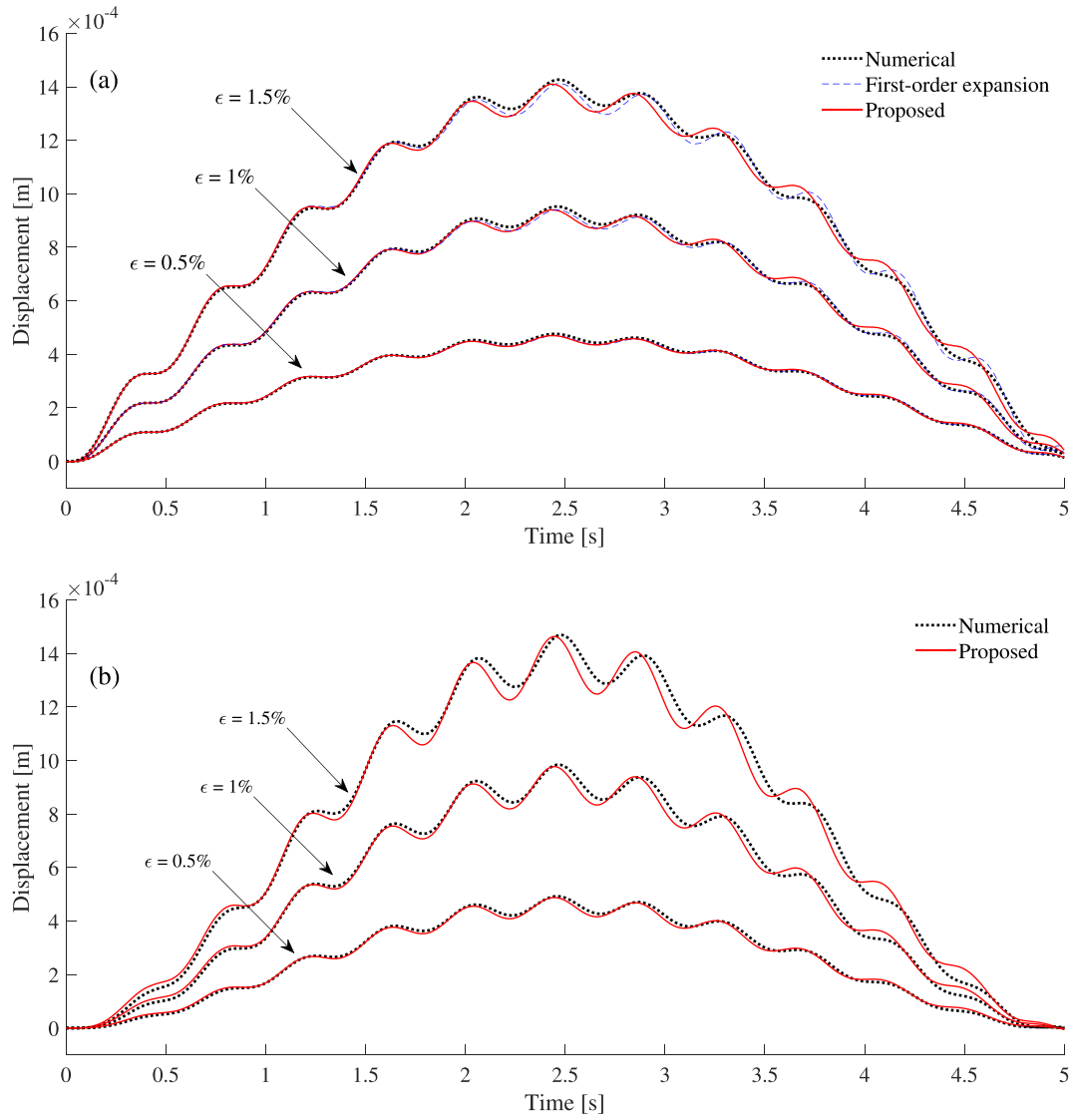


Fig. 7. Response for several values of the mass ratio (beam with rotational springs): (a) Displacement response of the mid-span of the beam; (b) Displacement response of the moving oscillator.

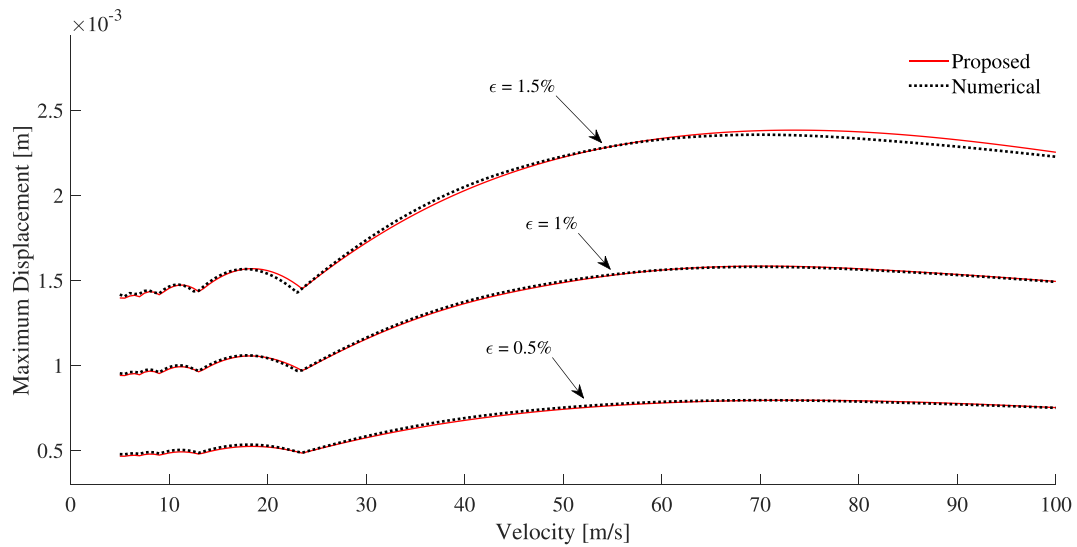


Fig. 8. Maximum displacement of the beam with rotational springs, as a function of the velocity for various values of the mass ratio.

stant, although the accuracy of the involved approximation tends to increase for higher spring stiffness.

4.3. Beam with general boundary conditions

As a last example, consider the case of an oscillator moving on a beam connected at the left-end with a vertical spring (spring constant  $k_1 = 10^9 \text{ kN/m}$ ) and a rotational spring (spring constant  $r_1 = 10^9 \text{ kN/rad}$ ), while the right-end is simply-supported, that is  $k_2 \rightarrow \infty$  and  $r_2 = 0$ . This case is examined to assess the reliability and applicability of the proposed procedure in dealing with more challenging BCs. Note that, as previously mentioned, particular attention should be paid to the initial condition of the beam, to appropriate capture the effect caused by the arrival of the moving oscillator on the left flexible support (see [28] for further details). In this example, the moving oscillator reach the left-end of the beam at the beginning of the observation, then crosses the beam and suddenly leaves it after reaching the right-end. Therefore, in this case, due to equilibrium condition, a jump in the acceleration response of the beam is generated in ( $t = 0$ ). Further, as far as the

first mode shape in Eq. (27) is concerned, this is reported in Eq. (A.11) in the Appendix A.

In Fig. 10 the displacement response of the mid-span of the beam and of the oscillator are shown. Specifically, in Fig. 10(a) the first-order expansion solution Eq. (55) (blue dashed line) is compared with the numerical solution of Eq. (18) (black dots), and the results of the approximate analytical solution in Eq. (39) (red line). Analogous results are reported in Fig. 10(b) for the response of the moving oscillator.

As it can be observed in these figures, results of the proposed approach closely follow the numerical solution of the complete system, and the FEM data, especially in terms of beam displacement. Further, again observe that the approximate analytical solution in Eq. (39) leads to sufficiently accurate results, although clearly Eq. (55) yields a more precise solution.

In addition, analyses have been carried out for different values of the mass ratio  $\varepsilon$ , again keeping constant the value of the frequency of the moving oscillator  $\omega_p$ . Pertinet results are reported in Fig. 11, where approximate analytical expressions (red line) are juxtaposed to the data of the numerical solutions of the complete system in Eqs. (18) (black dots).

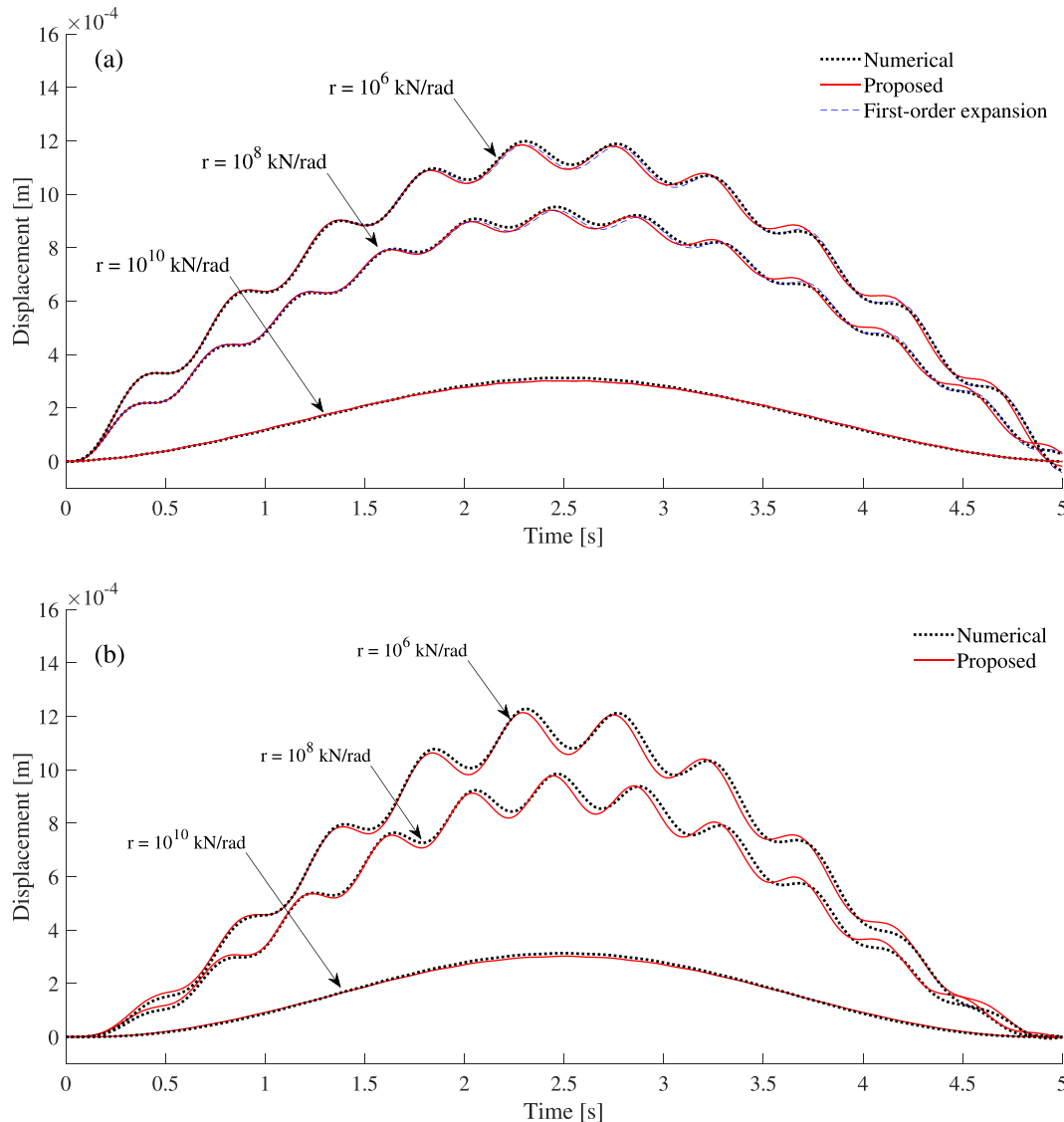
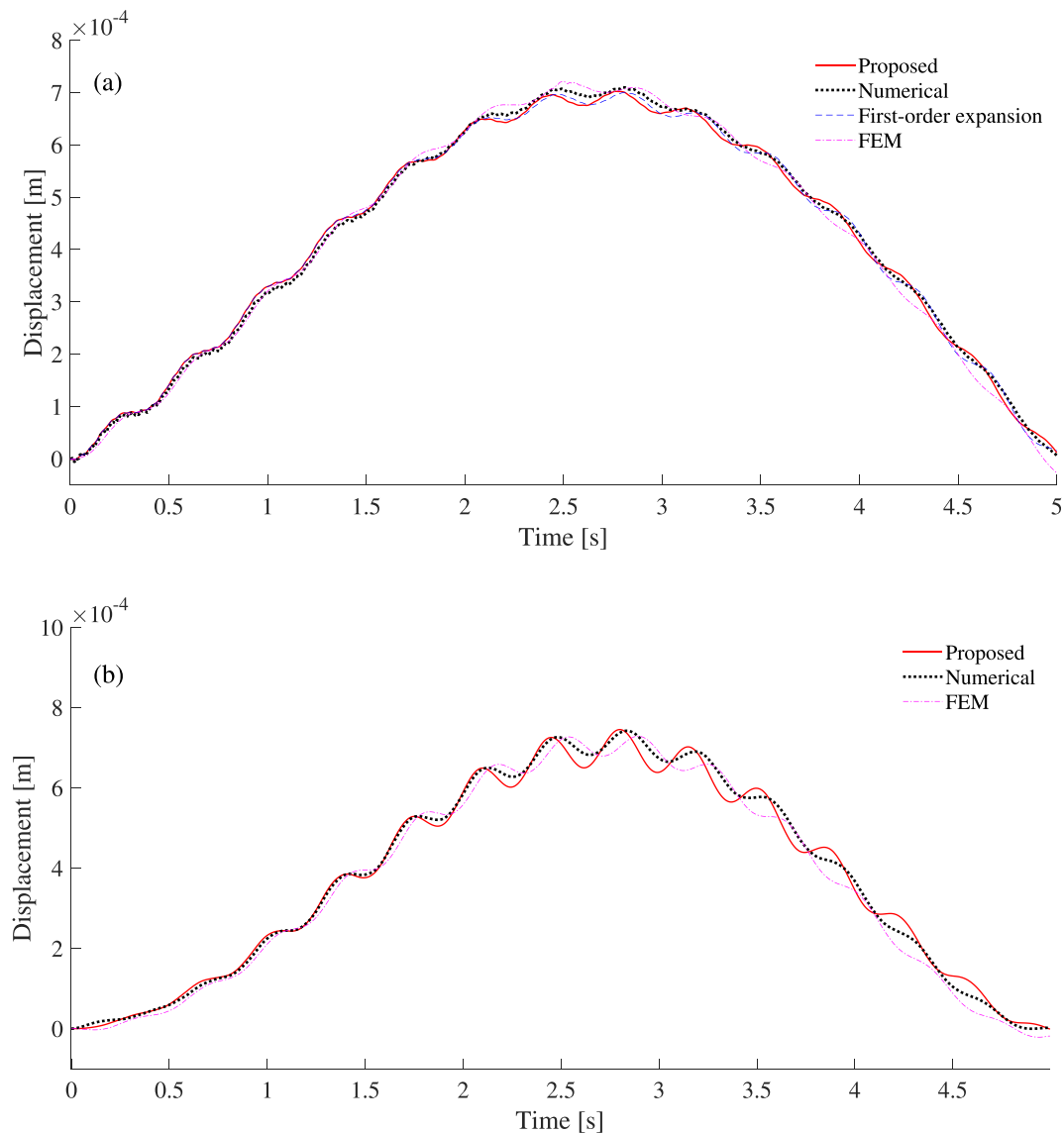


Fig. 9. Response for several values of spring stiffness (beam with rotational springs): (a) Displacement response of the mid-span of the beam; (b) Displacement response of the moving oscillator.



**Fig. 10.** Analysis for the case of a beam with general BCs: (a) Displacement response of the mid-span of the beam; (b) Displacement response of the moving oscillator.

As it can be seen in this figure, the proposed approximate analytical solution can generally capture the behavior of the response of the system for lower values of  $\varepsilon$ , especially in terms of beam displacements. From these analyses it can be argued that the considered approximate approach, and the related closed-form solutions, could be generally used for oscillator-beam mass ratio  $\varepsilon$  lower than 1%. If higher values of  $\varepsilon$  are employed, numerical solutions or higher-order expansions would be required when the response of the displacement of the moving oscillator is of concern.

Further, in Fig. 12 the maximum absolute displacement of the beam is reported as a function of the velocity of the moving oscillator, for several values of mass ratio. As it can be seen, again the proposed approximate analytical solution in Eq. (39) leads to almost the same results of Eqs. (18) for all the values of  $\varepsilon$ , thus further assessing the accuracy of the approach.

Finally, to assess the validity of the proposed approach for different degree of stiffness of the BCs, additional analyses have been performed varying the vertical and rotational springs' constants. In this regard, pertinent results are shown in Fig. 13, where analytical solutions (red lines) are juxtaposed with the numerical results of the complete system in Eqs. (18) (black dots).

Figures show that the approximate analytical solutions mostly follow the numerical results for all the analyzed cases. Clearly, however, the accuracy of the involved approximation tends to increase for higher spring stiffness, again leading to less accurate results when low values of spring stiffness are employed, especially in terms of the moving oscillator's displacement.

## 5. Concluding remarks

In this paper, a novel procedure is introduced for the determination of approximate closed-form expressions for the response of beams endowed with general boundary conditions (BCs) and subjected to a moving oscillator. Solutions are derived for both the beam and the moving oscillator displacements in time-domain. In this regard, the classical Euler-Bernoulli beam model is assumed, and the effects of damping in both the beam and the oscillator are taken into account. Note that these expressions have been obtained decoupling the originally coupled set of differential equations governing the response of the system. Specifically, this has been accomplished approximately representing the solution as

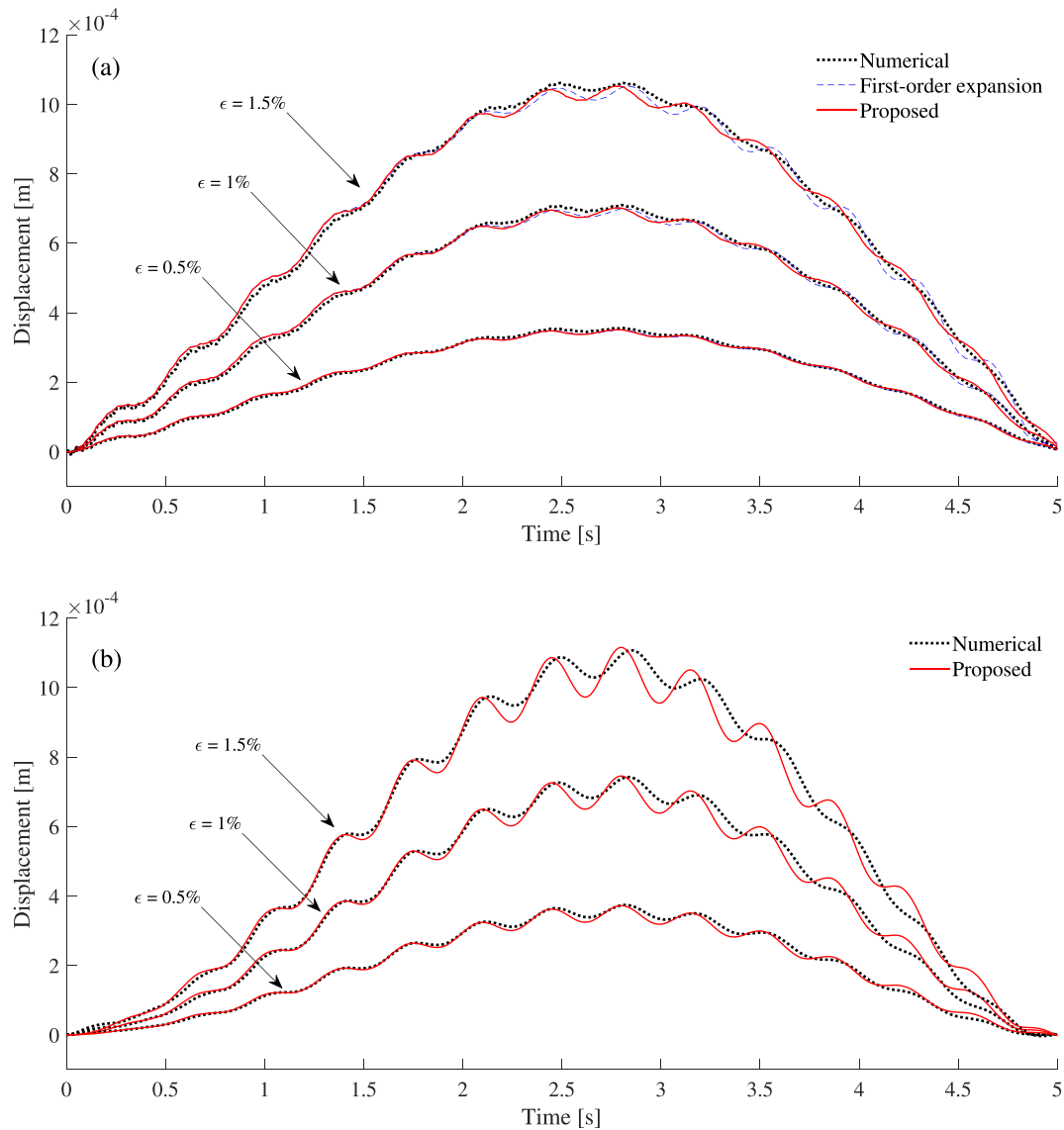


**Fig. 11.** Response for several values of the mass ratio (beam with general BCs): (a) Displacement response of the mid-span of the beam; (b) Displacement response of the moving oscillator.

an expansion in terms of powers of the beam-oscillator mass ratio, which is a generally small parameter. Further, the presence of general BCs has been treated appropriately exploiting the use of mode-shape functions of polynomial type, referred to as characteristic orthogonal polynomial. In this manner, the coefficients of the polynomials explicitly appear in the obtained analytical expressions, thus rendering the application of the proposed approach particularly straightforward for any chosen BC. On this base, closed-form expression of the response of the system have been derived for the zero-order expansion, which could be used to implement higher-order solutions useful when larger masses of the moving oscillator are employed.

Applications to three different possible cases of beam BCs have been considered, and analyses have been carried out for several values of systems parameters, including different values of mass ratio and velocity of the moving oscillator. The validity of the involved approximations is addressed for the different analyzed cases. Further, the comparison of the displacement responses determined by the proposed approach vis-à-vis pertinent data obtained numerically solving the original set of coupled differential equations, and

data of finite element analyses developed in a commercial software, has demonstrated the accuracy and reliability of the proposed analytical expressions. As expected, results have shown that the accuracy of the proposed approach increases for smaller values of the mass ratio, since this represents the main involved assumption of the procedure. Specifically, for all the analyzed cases, it has been seen that proposed approximate analytical solutions agree reasonably well with numerical results for mass ratio smaller than 1%. However, the accuracy may also vary depending on the selected BCs, especially if flexible supports are adopted.

Clearly, the proposed procedure offers significant advantages in determining efficiently, albeit approximately, the responses of the beam-moving oscillator system. Further, considering the non-negligible computational cost involved in the numerical integration of the original equation of motions, the herein presented solutions could be exploited for performing computationally efficient stochastic analysis when the irregular road profile is modelled as a stochastic process. Lastly, analytical solutions in frequency-domain could be also determined, which can be leveraged for instance in the context of the modern techniques of structural

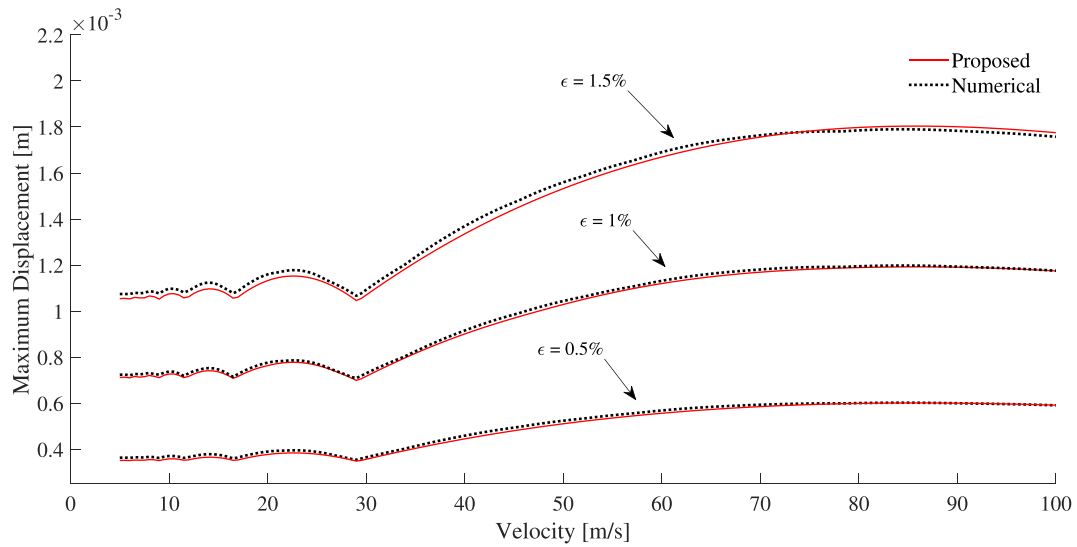


Fig. 12. Maximum displacement of the beam with general BCs, as a function of the velocity for various values of the mass of the moving oscillator.

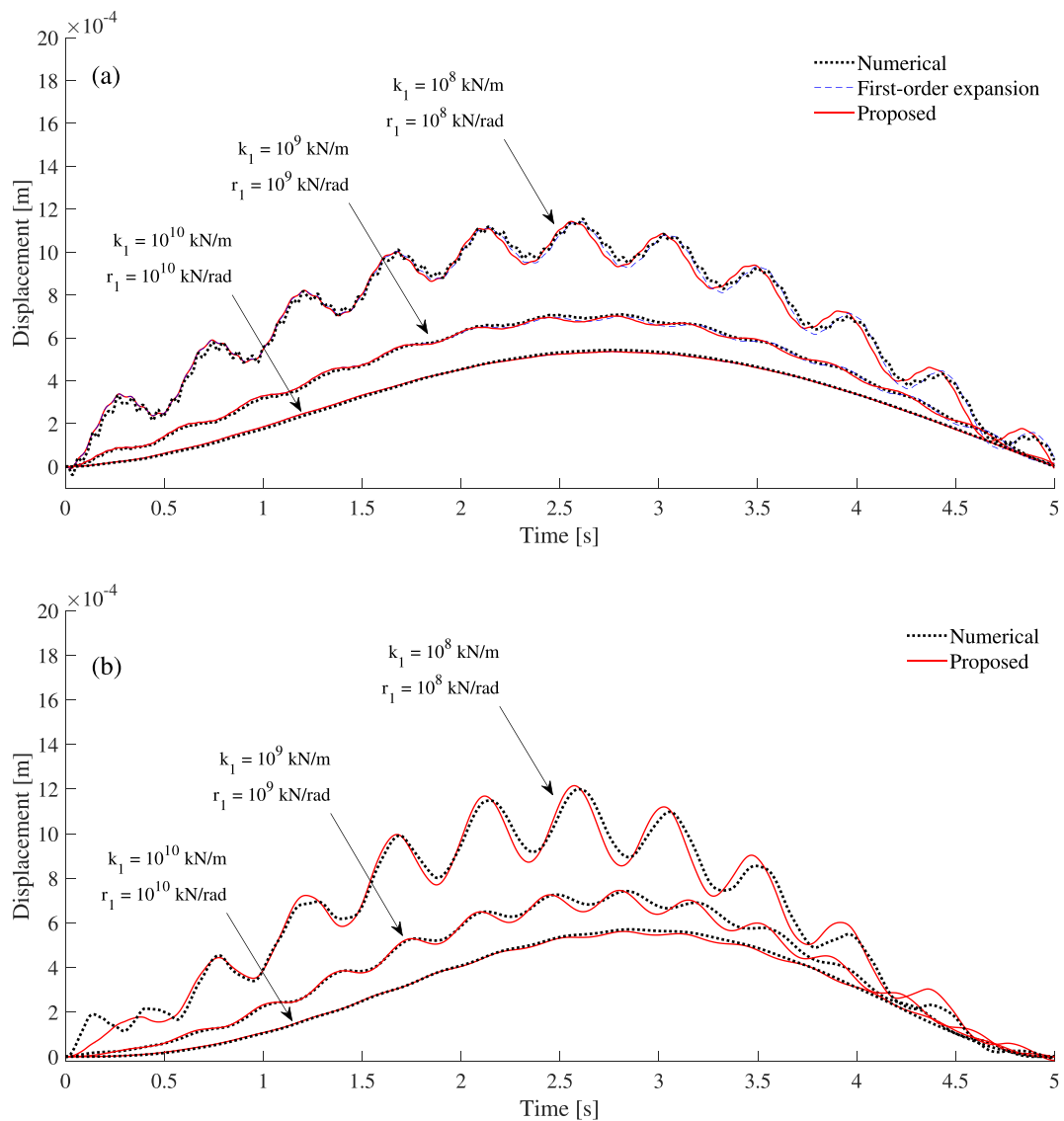


Fig. 13. Response for several values of spring stiffness (beam with general BCs): (a) Displacement response of the mid-span of the beam; (b) Displacement response of the moving oscillator.



health monitoring based on the vehicle-bridge interaction approach.

**Data availability**

Data will be made available on request.

**Declaration of Competing Interest**

The authors declare that they have no known competing financial interests or personal relationships that could have appeared to influence the work reported in this paper.

**Acknowledgements**

A. Di Matteo gratefully acknowledges the financial support of the project PO FESR 2014–2020 Crowdsense, and the support received from the Italian Ministry of University and Research, through the PRIN 2017 funding scheme (project 2017J4EAYB 002–Multiscale Innovative Materials and Structures “MIMS”).

**Appendix A. Determination of the first mode shape for general BCs**

In this appendix, the procedure described in [42] to determine the first element of the COPs is briefly reported and applied to the considered case of general BCs.

In this regard, the first member polynomial in the orthogonal set is constructed so as to satisfy both the geometrical and natural BCs of the beam. To this aim, considering the transformation of variable  $x = \xi/L$ , the BCs in Eq. (13) becomes

$$\begin{aligned} -\tilde{k}_1 \phi_j(0) &= \phi_j'''(0) \\ \tilde{r}_1 \phi_j'(0) &= \phi_j''(0), \end{aligned} \tag{A.1}$$

for the left boundary ( $\xi = 0$ ), and

$$\begin{aligned} \tilde{k}_2 \phi_j(1) &= \phi_j'''(1) \\ -\tilde{r}_2 \phi_j'(1) &= \phi_j''(1) \end{aligned} \tag{A.2}$$

for the right boundary ( $\xi = 1$ ), where  $\tilde{r}_p = r_p L/EI$  and  $\tilde{k}_p = k_p L^3/EI$ , with  $p$  being 1 or 2 (for left and right end, respectively).

Assuming the first beam mode shape as a fourth-degree polynomial as in Eq. (26), that is

$$\varphi_1(\xi) = a_{1,0} + a_{1,1}\xi + a_{1,2}\xi^2 + a_{1,3}\xi^3 + a_{1,4}\xi^4 \tag{A.3}$$

and applying the BCs in Eqs. (A.1) and (A.2), gives the mode shape coefficients as

$$\begin{aligned} a_{1,1} &= a_{1,0} \\ &\times \frac{\tilde{k}_1 \left( 72 + 48\tilde{r}_2 + 6\tilde{k}_2 \right) - 24\tilde{k}_2 \left( 3 + \tilde{r}_2 \right) + \tilde{k}_1 \tilde{k}_2 \tilde{r}_2}{6 \left[ 3\tilde{k}_2 \left( 4 + \tilde{r}_2 \right) + \tilde{r}_1 \tilde{k}_2 \left( 5 + \tilde{r}_2 \right) + 24 \left( \tilde{r}_1 + \tilde{r}_2 + \tilde{r}_1 \tilde{r}_2 \right) \right]} \end{aligned} \tag{A.4}$$

$$\begin{aligned} a_{1,2} &= a_{1,0} \frac{\tilde{r}_1}{12} \\ &\times \frac{\tilde{k}_1 \left( 72 + 48\tilde{r}_2 + 6\tilde{k}_2 \right) - 24\tilde{k}_2 \left( 3 + \tilde{r}_2 \right) + \tilde{k}_1 \tilde{k}_2 \tilde{r}_2}{\left[ 3\tilde{k}_2 \left( 4 + \tilde{r}_2 \right) + \tilde{r}_1 \tilde{k}_2 \left( 5 + \tilde{r}_2 \right) + 24 \left( \tilde{r}_1 + \tilde{r}_2 + \tilde{r}_1 \tilde{r}_2 \right) \right]} \end{aligned} \tag{A.5}$$

$$a_{1,3} = -a_{1,0} \frac{\tilde{k}_1}{6} \tag{A.6}$$

$$\begin{aligned} a_{1,4} &= a_{1,0} \\ &\times \frac{\tilde{k}_1 \left[ 4\tilde{k}_2 \left( 3 + \tilde{r}_1 \right) + \tilde{r}_2 \tilde{k}_2 \left( 4 + \tilde{r}_1 \right) \right] + 12 \left( \tilde{k}_1 + \tilde{k}_2 \right) \left( \tilde{r}_1 + \tilde{r}_2 + \tilde{r}_1 \tilde{r}_2 \right)}{12 \left[ 3\tilde{k}_2 \left( 4 + \tilde{r}_2 \right) + \tilde{r}_1 \tilde{k}_2 \left( 5 + \tilde{r}_2 \right) + 24 \left( \tilde{r}_1 + \tilde{r}_2 + \tilde{r}_1 \tilde{r}_2 \right) \right]} \end{aligned} \tag{A.7}$$

Further, the first coefficient  $a_{1,0}$  can be found using the normalization condition in Eq. (17), that in this case becomes

$$\int_0^1 \varphi_1^2(\xi) d\xi = 1 \tag{A.8}$$

In this manner, substituting the pertinent values of the spring stiffness coefficients in Eqs. (A.4–A.8), all the various mode shape functions can be determined.

For instance, the first mode shape of a simply-supported beam can be obtained assuming  $\tilde{k}_1 = \tilde{k}_2 \rightarrow \infty$  and  $\tilde{r}_1 = \tilde{r}_2 = 0$ . Substituting these values in Eqs. (A.4–A.8), and taking into account Eq. (30), the mode shape in Eq. (31) is

$$\varphi_1(x) = \frac{3}{L^4} \sqrt{\frac{70}{31}} x \left( L^3 - 2Lx + x^3 \right) \tag{A.9}$$

Analogously, assuming  $\tilde{k}_1 = \tilde{k}_2 \rightarrow \infty$  and  $\tilde{r}_1 = \tilde{r}_2 = \tilde{r}$ , the case of a beam with rotational springs at both ends can be determined as

$$\varphi_1(x) = \frac{3\sqrt{70}}{L^4 (2 + \tilde{r})} \left[ \frac{124 + 22\tilde{r} + \tilde{r}^2}{(2 + \tilde{r})^2} \right]^{-\frac{1}{2}} (L - x)x \left[ 2L^2 + (2 + \tilde{r})x(L - x) \right] \tag{A.10}$$

Finally, the case of a beam connected at the left-end with a vertical and a rotational spring, and simply-supported at the right-end ( $\tilde{k}_2 \rightarrow \infty, \tilde{r}_2 = 0$ ), is given as

$$\begin{aligned} \varphi_1(x) &= C(L - x) \left[ 1 + \frac{\left( \tilde{k}_1 + 5\tilde{r}_1 \right)}{L \left( 12 + 5\tilde{r}_1 \right)} x + \frac{\left( -2\tilde{r}_1 + 2\tilde{k}_1 + \tilde{k}_1 \tilde{r}_1 \right)}{2L^2 \left( 12 + 5\tilde{r}_1 \right)} \right. \\ &\quad \left. x^2 - \frac{\left( 3\tilde{r}_1 + 3\tilde{k}_1 + \tilde{k}_1 \tilde{r}_1 \right)}{3L^3 \left( 12 + 5\tilde{r}_1 \right)} x^3 \right] \end{aligned} \tag{A.11}$$

where  $C$  is a constant that can be found using Eq. (17).

**Appendix B. Determination of the displacement response of the moving oscillator**

In this appendix, the terms required to initialize the recursive relation in Eq. (51) are reported. Specifically, evaluating Eq. (50.a) for  $k = 0$ , Eq. (51) leads to the following expression

$$\begin{aligned} I_{j,0,s}^{(1)}(t) &= -\frac{2\zeta_j \omega_j}{\delta_j} \tilde{I}_{j,s}(t) - \frac{1}{\delta_j} \left[ \tilde{I}_{j,s}(t) - s \tilde{I}_{j,s-1}(t) \right] + \frac{1}{\delta_j} \theta_{y,s}(t); \quad s \\ &\geq 1 \end{aligned} \tag{B.1}$$

where

$$\tilde{I}_{j,s}(t) = \int_0^t h_y(t - \tau) \tau^s h_j(\tau) d\tau \tag{B.2}$$

After several manipulations, Eq. (B.2) leads to

$$\begin{aligned} \tilde{I}_{j,s}(t) = & \frac{\Gamma(1+s)}{4\omega_{dj}\omega_{d,v}} \left[ e^{-t\sigma_v} \left( \bar{\eta}_1^{-1-s} - \bar{\eta}_2^{-1-s} \right) + e^{-t\bar{\sigma}_v} \left( \bar{\eta}_1^{-1-s} - \bar{\eta}_2^{-1-s} \right) \right] + \\ & \frac{1}{4\omega_{dj}\omega_{d,v}} \left[ e^{-t\sigma_v} \left( \bar{\eta}_2^{-1-s} \Gamma(1+s, \eta_2 t) - \bar{\eta}_1^{-1-s} \Gamma(1+s, \bar{\eta}_1 t) \right) - \right. \\ & \left. e^{-t\bar{\sigma}_v} \left( \bar{\eta}_1^{-1-s} \Gamma(1+s, \eta_1 t) - \bar{\eta}_2^{-1-s} \Gamma(1+s, \bar{\eta}_2 t) \right) \right] \end{aligned} \quad (B.3)$$

in which  $\sigma_v = \zeta_v \omega_v + i\omega_{d,v}$ ,  $\eta_1 = \zeta_j \omega_j - \zeta_v \omega_v + i(\omega_{d,j} + \omega_{d,v})$ ,  $\eta_2 = \zeta_j \omega_j - \zeta_v \omega_v + i(\omega_{d,j} - \omega_{d,v})$ , and the overbar stands for complex conjugate.

Next, evaluating Eq. (B.1) for  $s = 0$  yields

$$I_{j,0,0}^{(1)}(t) = -\frac{1}{\delta_j} \left[ 2\zeta_j \omega_j \tilde{I}_{j,0}(t) + \tilde{I}_{j,s}(t) \right] + \frac{1}{\delta_j} \theta_{y,0}(t) \quad (B.4)$$

where

$$\theta_{y,0}(t) = -\frac{1}{\delta_v} \left[ 2\zeta_v \omega_v h_y(t) + \dot{h}_y(t) \right] + \frac{1}{\delta_v} \quad (B.5)$$

and  $\delta_v = \zeta_v^2 \omega_v^2 + \omega_{d,v}^2$ . Finally, evaluating Eq. (50.a) for  $s = 0$ , Eq. (51) leads to

$$I_{j,k,0}^{(1)}(t) = -\frac{k}{\delta_j} \left[ 2\zeta_j \omega_j I_{j,k-1,0}^{(1)}(t) + \dot{I}_{j,k-1,0}^{(1)}(t) \right] + \frac{1}{\delta_j} \theta_{y,k}(t); \quad k \geq 1 \quad (B.6)$$

where,  $\theta_{y,k}(t)$  given as in Eq. (52), can be expressed directly as

$$\theta_{y,k}(t) = -\frac{k}{\delta_v} \left[ 2\zeta_v \omega_v \theta_{y,k-1}(t) + \dot{\theta}_{y,k-1}(t) \right] + \frac{t^k}{\delta_v}; \quad k \geq 1 \quad (B.7)$$

In this manner, the above reported equations can be employed to find the expression of the function  $I_{j,k,s}^{(1)}(t)$  through a recursive use of Eq. (51), and thus the solution of the oscillator displacement in Eq. (49).

**References**

[1] Fryba L. *Vibration of solids and structures under moving loads*. 3rd ed. Thomas Telford; 1999.

[2] Yang Y, Yau J, Wu Y. *Vehicle-bridge interaction dynamics*. World Scientific Publishing Company Incorporated; 2004.

[3] Ouyang H. *Moving-load dynamic problems: a tutorial (with a brief overview)*. Mech Syst Signal Process 2011;25(6):2039–60.

[4] Rao G. *Linear dynamics of an elastic beam under moving loads*. J Vib Acoust 2000;122(3):281–9.

[5] Dugush Y, Eisenberger M. *Vibrations of non-uniform continuous beams under moving loads*. J Sound Vib 2002;254(5):911–26.

[6] Henchi K, Fafard M, Dhatt G, Talbot M. *Dynamic behaviour of multi-span beams under moving loads*. J Sound Vib 1997;199(1):33–50.

[7] Greco A, Santini A. *Dynamic response of a flexural non-classically damped continuous beam under moving loadings*. Comput Struct 2002;80(26):1945–53.

[8] Di Lorenzo S, Di Paola M, Failla G, Pirrotta A. *On the moving load problem in Euler-Bernoulli uniform beams with viscoelastic supports and joints*. Acta Mech 2017;228:805–21.

[9] Svedholm C, Zangeneh A, Pacoste C, François S, Karoumi R. *Vibration of damped uniform beams with general end conditions under moving loads*. Eng Struct 2016;126:40–52.

[10] Johansson C, Pacoste C, Karoumi R. *Closed-form solution for the mode superposition analysis of the vibration in multi-span beam bridges caused by concentrated moving loads*. Comput Struct 2013;119:85–94.

[11] Yang YB, Lin CW. *Vehicle-bridge interaction dynamics and potential applications*. J Sound Vib 2005;284:205–26.

[12] Akin JE, Mofid M. *Numerical solution for response of beams with moving mass*. J Struct Eng 1989;115(1):120–31.

[13] Lee HP. *Dynamic response of a beam with a moving mass*. J Sound Vib 1996;191(2):289–94.

[14] Michaltsos G, Sophianopoulos D, Kounadis A. *The effect of a moving mass and other parameters on the dynamic response of a simply supported beam*. J Sound Vib 1996;191(3):357–62.

[15] Ahmadi M, Nikkhoo A. *Utilization of characteristic polynomials in vibration analysis of nonuniform beams under a moving mass excitation*. Appl Math Model 2014;38:2130–40.

[16] Pesterev AV, Bergman LA. *Response of elastic continuum carrying moving linear oscillator*. J Eng Mech 1997;123:878–84.

[17] Pesterev AV, Bergman LA. *An improved series expansion of the solution to the moving oscillator problem*. J Vib Acoustics 2000;122:54–61.

[18] Muscolino G, Palmeri A, Sofi A. *Absolute versus relative formulations of the moving oscillator problem*. Int J Solids Struct 2009;46:1085–94.

[19] Stancioiu D, Ouyang H, Motterhead JE. *Vibration of a beam excited by a moving oscillator considering separation and reattachment*. J Sound Vib 2008;10:1128–40.

[20] Yang YB, Wu YS. *A versatile element for analyzing vehicle-bridge interaction response*. Eng Struct 2001;23:452–69.

[21] Biondi B, Muscolino G. *Component-mode synthesis method for coupled continuous and FE discretized substructures*. Eng Struct 2003;25:419–33.

[22] Biondi B, Muscolino G, Sofi A. *A substructure approach for the dynamic analysis of train-trackbridge interaction*. Comput Struct 2005;83:2271–81.

[23] Kwasniewski L, Li H, Wekezer J, Malachowski J. *Finite element analysis of vehicle-bridge interaction*. Finite Elem Anal Des 2006;42:950–9.

[24] Salcher P, Adam C. *Modeling of dynamic train-bridge interaction in high-speed rail-ways*. Acta Mech 2015;226(8):2473–95.

[25] Yang YB, Yau J. *Vertical and pitching resonance of train cars moving over a series of simple beams*. J Sound Vib 2015;337:135–49.

[26] Liu K, De Roock G, Lombaer G. *The effect of dynamic train-bridge interaction on the bridge response during a train passage*. J Sound Vib 2009;325:240–51.

[27] Yang YB, Zhang B, Wang T, Wu Y. *Two-axle test vehicle for bridges: theory and applications*. Int J Mech Sci 2019;152:51–62.

[28] Hirzinger B, Adam C, Salcher P. *Dynamic response of a non-classically damped beam with general boundary conditions subjected to a moving mass-spring-damper system*. Int J Mech Sci 2020;185:105877.

[29] Stoura CD, Dimitrakopoulos EG. *A Modified Bridge System method to characterize and decouple vehicle-bridge interaction*. Acta Mechanica 2020;231:3825–45.

[30] Stoura CD, Dimitrakopoulos EG. *MDOF extension of the Modified Bridge System method for vehicle-bridge interaction*. Nonlinear Dyn 2020;102:2103–23.

[31] Zhu XW, Law SS. *Structural health monitoring based on vehicle-bridge interaction: accomplishments and challenges*. Advances Struct Eng 2015;18:1999–2015.

[32] Lin CW, Yang YB. *Use of a passing vehicle to scan the fundamental bridge frequencies: An experimental verification*. Eng Struct 2005;27:1865–78.

[33] Yang YB, Chen WF, Yu HW, Chan CS. *Experimental study of a hand-drawn cart for measuring the bridge frequencies*. Eng Struct 2013;57:222–31.

[34] Yang YB, Chang KC. *Extraction of bridge frequencies from the dynamic response of a passing vehicle enhanced by the EMD technique*. J Sound Vib 2009;322:718–39.

[35] Wang H, Nagayama T, Nakasuka T, Zhao B, Su D. *Extraction of bridge fundamental frequency from estimated vehicle excitation through a particle filter approach*. J Sound Vib 2018;428:44–58.

[36] Yang YB, Xu H, Zhang B, Xiong F, Wang ZL. *Measuring bridge frequencies by a test vehicle in non-moving and moving States*. Eng Struct 2020;203:109859.

[37] González A, Obrien EJ, McGetrick PJ. *Identification of damping in a bridge using a moving instrumented vehicle*. J Sound Vib 2012;331(18):4115–31.

[38] Yang YB, Li YC, Chang KC. *Constructing the mode shapes of a bridge from a passing vehicle: a theoretical study*. Smart Struct Syst 2014;13(5):797–819.

[39] Malekjafarian A, Obrien EJ. *Identification of bridge mode shapes using short time frequency domain decomposition of the responses measured in a passing vehicle*. Eng Struct 2014;81:386–97.

[40] Obrien EJ, Malekjafarian A. *A mode shape-based damage detection approach using laser measurement from a vehicle crossing a simply supported bridge*. Struct Control Health Monit 2016;23:1273–86.

[41] Nayfeh AH. *Perturbation Methods*. New York: Wiley-Interscience; 1973.

[42] Cheung YK, Chen SH, Lau SL. *A modified Lindstedt-Poincaré method for certain strongly non-linear oscillators*. Int J Non-Linear Mech 1991;26:367–78.

[43] Ozis T, Yildirim A. *Determination of limit cycles by a modified straightforward expansion for nonlinear oscillators*. Chaos Solitons Fractals 2006;32:445–8.

[44] Bhat RB. *Natural frequencies of rectangular plates using characteristic orthogonal polynomials in Rayleigh-Ritz method*. J Sound Vib 1985;102:493–9.

[45] Battaglia G, Di Matteo A, Micale G, Pirrotta A. *Vibration-based identification of mechanical properties of orthotropic arbitrarily shaped plates: Numerical and experimental assessment*. Compos Pt B-Eng 2018;150:212–25.

[46] Roberts JB, Spanos PD. *Random vibration and statistical linearization*. New York: Dover Publications; 2003.

[47] Di Matteo A, Spanos PD, Pirrotta A. *Approximate survival probability determination of hysteretic systems with fractional derivative elements*. Prob Eng Mech 2018;54:138–46.

[48] Di Matteo A, Pirrotta A, Gebel E. *Spanos Analysis of block random rocking on nonlinear flexible foundation*. Prob Eng Mech 2020;59:103017.

[49] Dodds CJ, Robson JD. *The description of road surface roughness*. J Sound Vib 1973;31:175–83.

[50] Abramowitz M, Stegun J. *Handbook of mathematical functions with formulas, graphs and mathematical tables*. New York: Dover Publications; 1963.